Club Español de Magnetismo, Asamblea Annual, Madrid, Diciembre, 2006

EFECTS AND MODELS OF INTERACTION OF MAGNETIC FIELDS WITH NEURONE MEMBRANE

A. del MORAL

Laboratorio de Magnetismo, Departamento de Física de Materia Condensada & Instituto de Ciencia de Materiales, Universidad de Zaragoza & CSIC, 50009 Zaragoza, Spain.

and

Laboratorio de Magnetobiología (*), Facultad de Medicina, Universidad de Zaragoza, 50009 Zaragoza, Spain

(*) In collaboration with Prof. María J. Azanza and Dr. Rodolfo Pérez-Bruzón.

Helix brain and **mapped** single neurones:

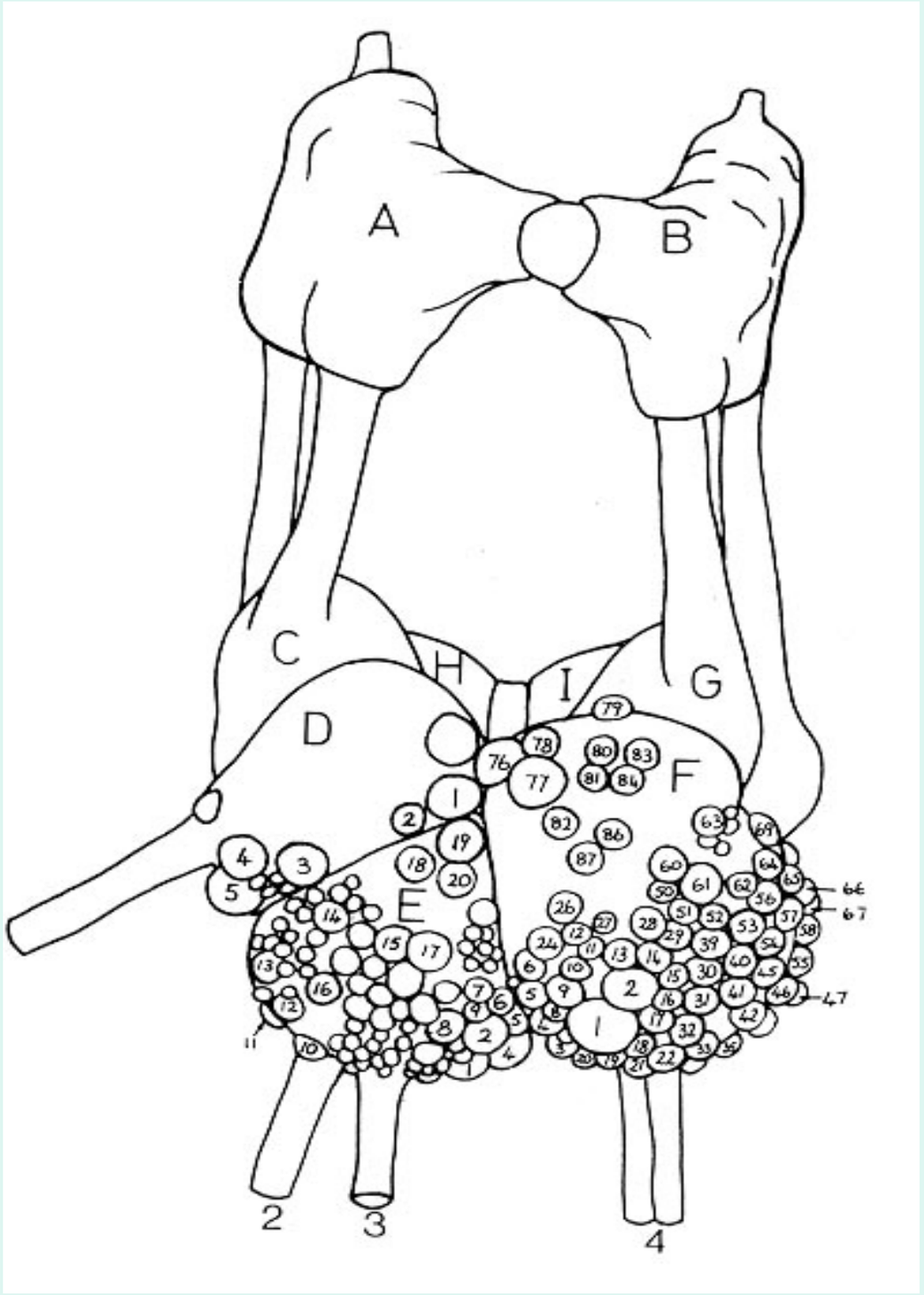

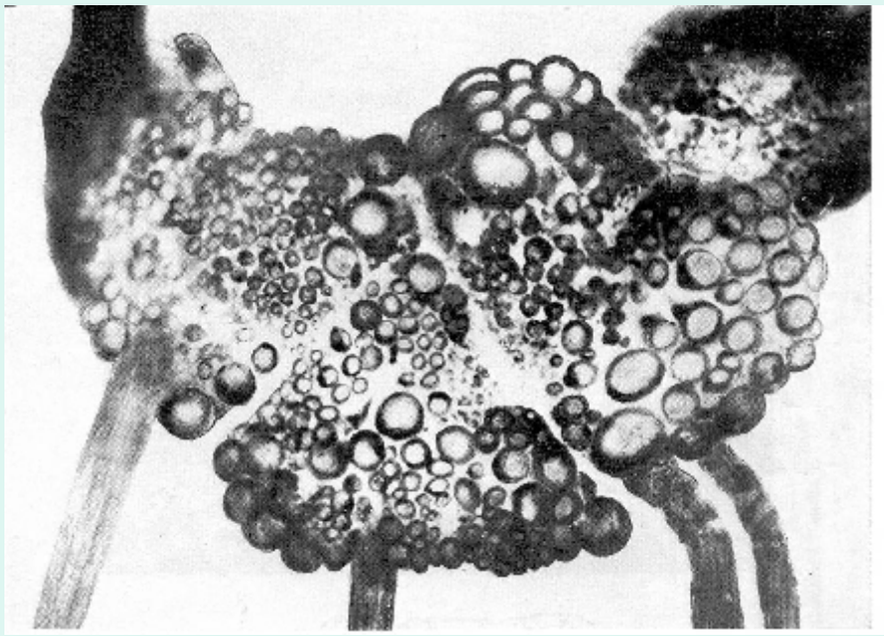

CONTENTS:

PART I.-

MODEL OF SUPERDIAMAGNETISM AND Ca^{2+} COULOMB EXPLOSION (SD+CE) FOR NEURONE MEMBRANE RESPONSES TO APPLIED MAGNETIC FIELDS.

PART II.-

MODELS OF NEURONE DYNAMICS: SPONTANEOUS AND UNDER ALTERNATING MAGNETIC FIELDS.

Contents Part I：

1.- Biological effects of MFs on neurones.

2.- The bases of SD+CE model and energetics of model.

3.- Magnetic field dependence of action potential frequency.

4.- Thermal effects.

5.- Action potential amplitude effect of MF: electrogenic pumps.

6.- Small neurone networks synchronization under ELF MF.

PART I.-

MODEL OF SUPERDIAMAGNETISM AND Ca^{2+} COULOMB EXPLOSION (SD+CE) FOR NEURONE MEMBRANE RESPONSES TO APPLIED MAGNETIC FIELDS.

In the **bioelectric** activity (dynamics) of neural tissue, either **spontaneous** or under **applied magnetic field** (MF) there appear two main issues:

i.- the **generation** and **structure** of the bioelectric impulse,

ii.- its repetition **frequency**.

♦*Biolectric impulse:*

- The process by which the impulse starts it is thought to be the result of small sub-threshold voltages sum up to a **threshold voltage**, V_s where the **depolarization (D)** process starts, with the **entrance of Na^{2+} ions** to the cell, through **voltage activated** Na^+-channels.

** We will discuss here the **time shape of the impulse** once it is formed, dividing it in: **depolarization (D)** and **hyperpolarization** (**H**, due to **sorting out of K^+ ions** through delayed rectifier voltage-operated K^+-channels).

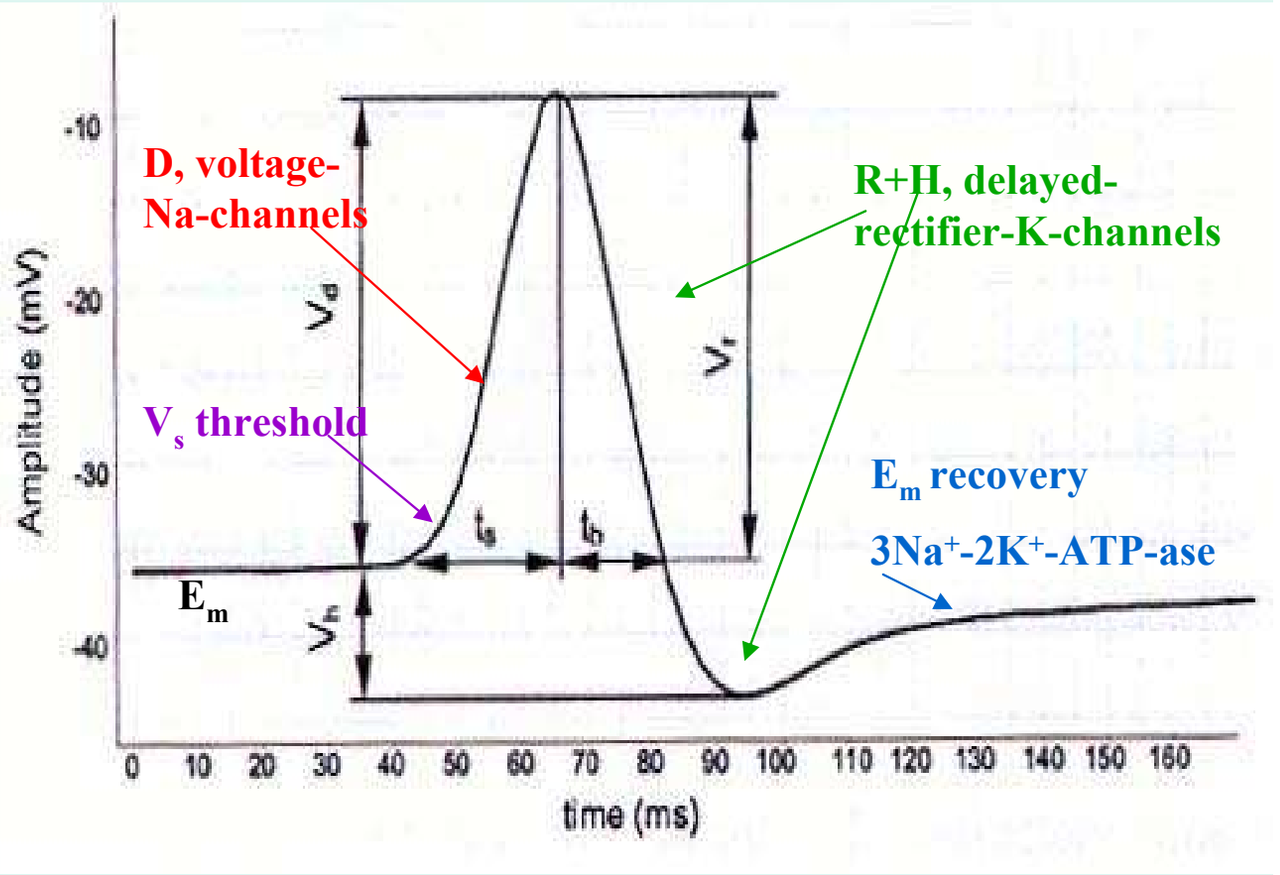

Fig.19.-

***The MF effect on **electrogenic pumps**,which promote the entrance of 2 K^+ ions against the sorting out of 3 Na^{2+} ions, making the membrane going to the **resting potential**, E_m was already considered in Part I, so completing the **full scenario**. The MF effect on such a regime is the **decrease** of impulse D amplitude, when MF is **strong** enough (2).

(2) Azanza M.J., and del Moral A., J. Magn. Magn. Mat. 157-158: 593-594, 1996.

A.- WHICH ARE THE BIOLOGICAL EFFECTS TO BE EXPLAINED?

- Effects of **static** magnetic fields (**SMF**) on ***single neurones***, to separate out MF from ***electric*** fields accompanying time rapidly variable magnetic fields.

- Understanding why **SMF** (B=1 mT -few kGauss) and ***quasistatic*** or **extremely low frequency (ELF)**, f_M electromagnetic fields (EMF), these of ***weaker*** intensity (from about 0.1 mT up to 10 mT and also down to **0.2μT**) are the relevant interacting ones with ***neurones*** (high frequencies (> 100 MHz) seem irrelevant).

- **Very elusive problem** since the main discovery of the so called "***frequency window effect***" made by Bawin and Adey since thirty years ago (1975, to be considered in Part II).

Our main experimental observations in ***Helix*** **single neurones**:

i) a progressive and strong **decrease** of the neuron **firing frequency** with increasing intensity of **SMF** from ≅ 10 G (1 mT) (Figs 1 and 2);

ii) a sharp **full abolishing** of neuron activity at SMF fields ≅ 5.7-7.3 kG (Figs.2, 3)

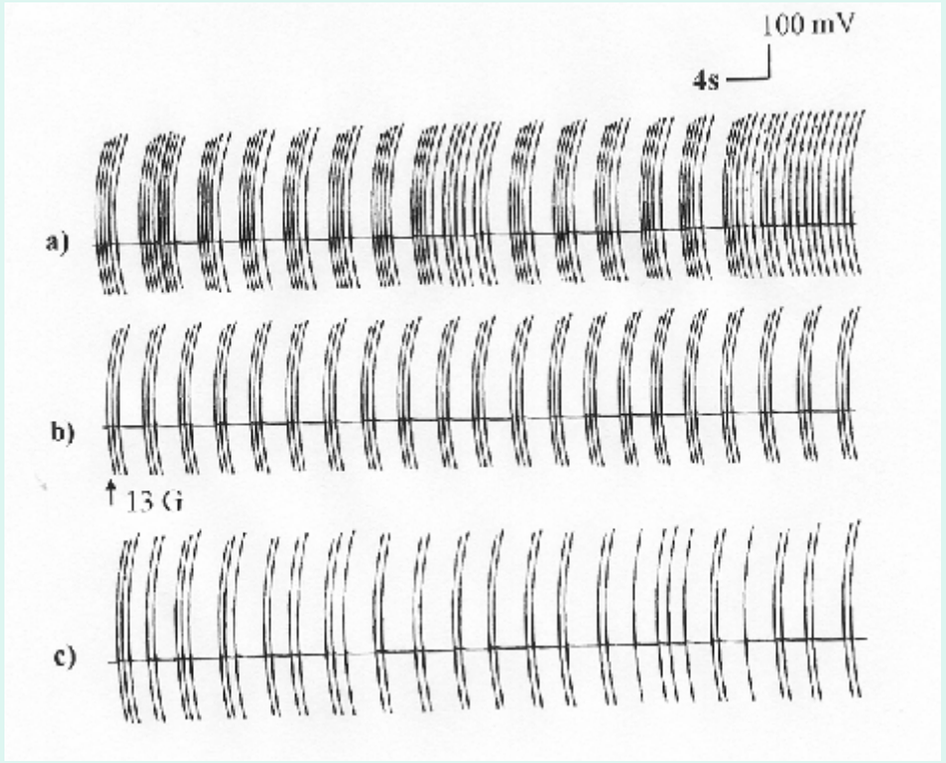

Fig. 1.- SMF B= 13 G. a) spontaneous, natural, bioelectric activity. b) and c) progressive firing frequency decreasing with H application.

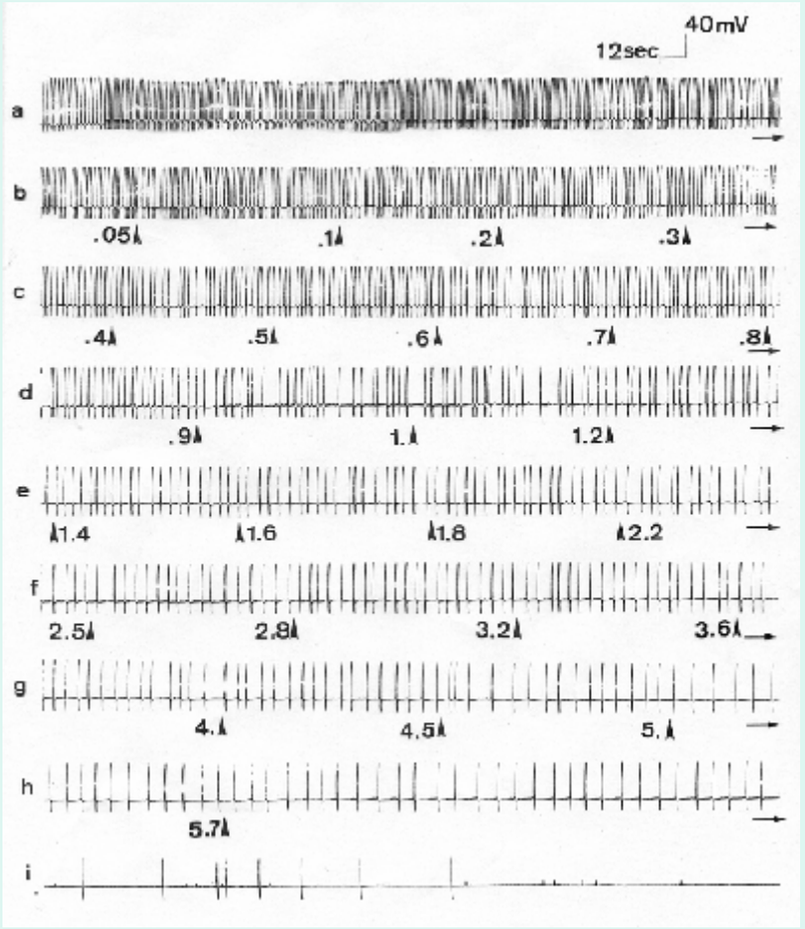

Fig.2.- SMF (0.05-5.7 kG range) induces a progressive decrease of neurone firing frequency: a) spontaneous activity. b) –h) MF intensity is progressively increased at steps of 1 min. i) abolishing of neuron activity

iii) progressive **decrease** of the **amplitude** spikes with increasing SMF B (Figs.2 and 3).

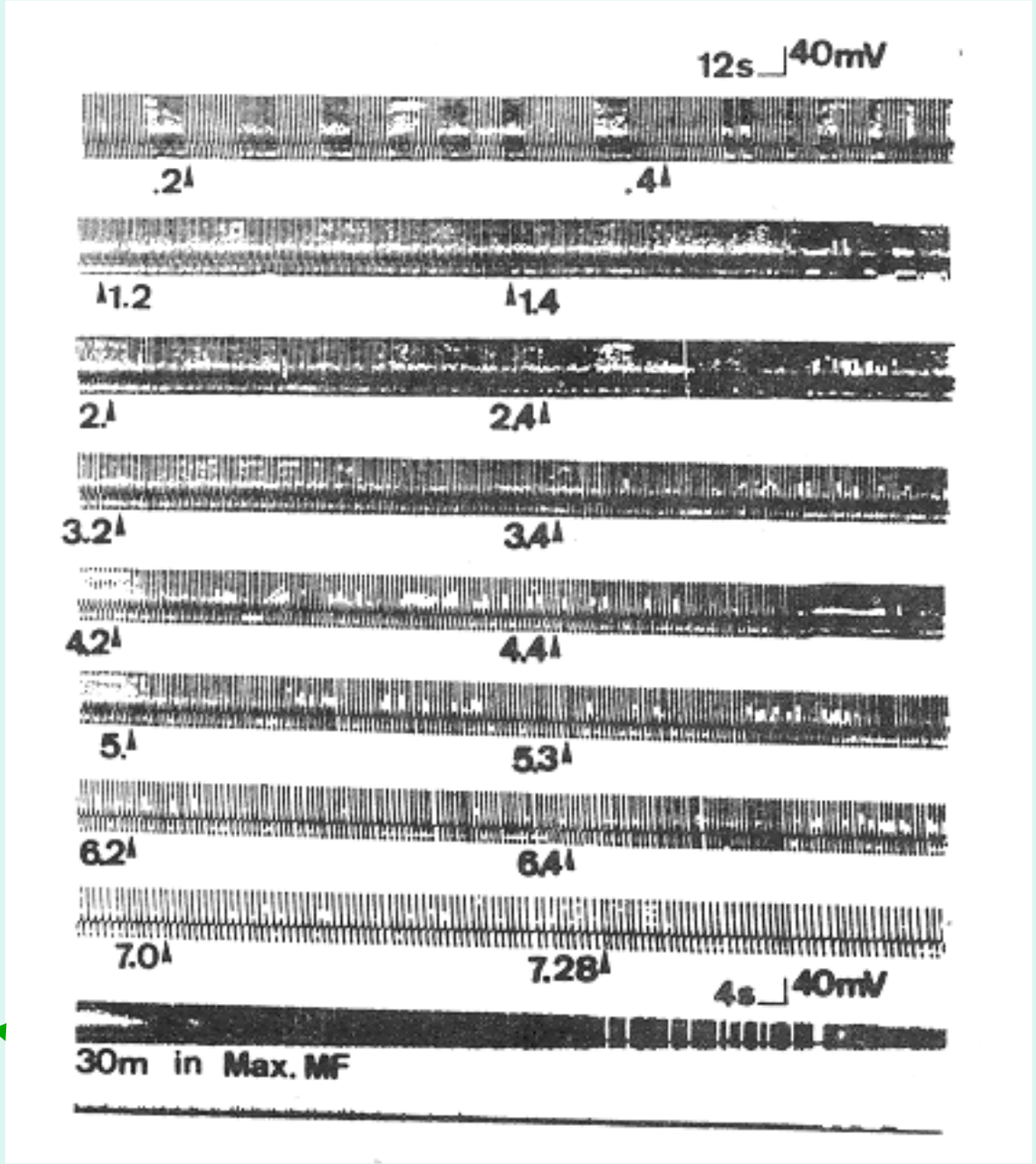

Fig.-3. SMF induces neuron depolarization voltage amplitude decrease. SMF intensity in *kGauss*.

In the last two recordings, after 30 min of exposure to 7.2 kG SMF, the spikes amplitude was ***completely abolished*****.**

iv) ♠ Under ELF-MF we found ***synchronization*** firing of couples of neurons.
♠♠Synaptic delay is not observed, favouring our SD+CE model via PP electric quadrupolar interaction.

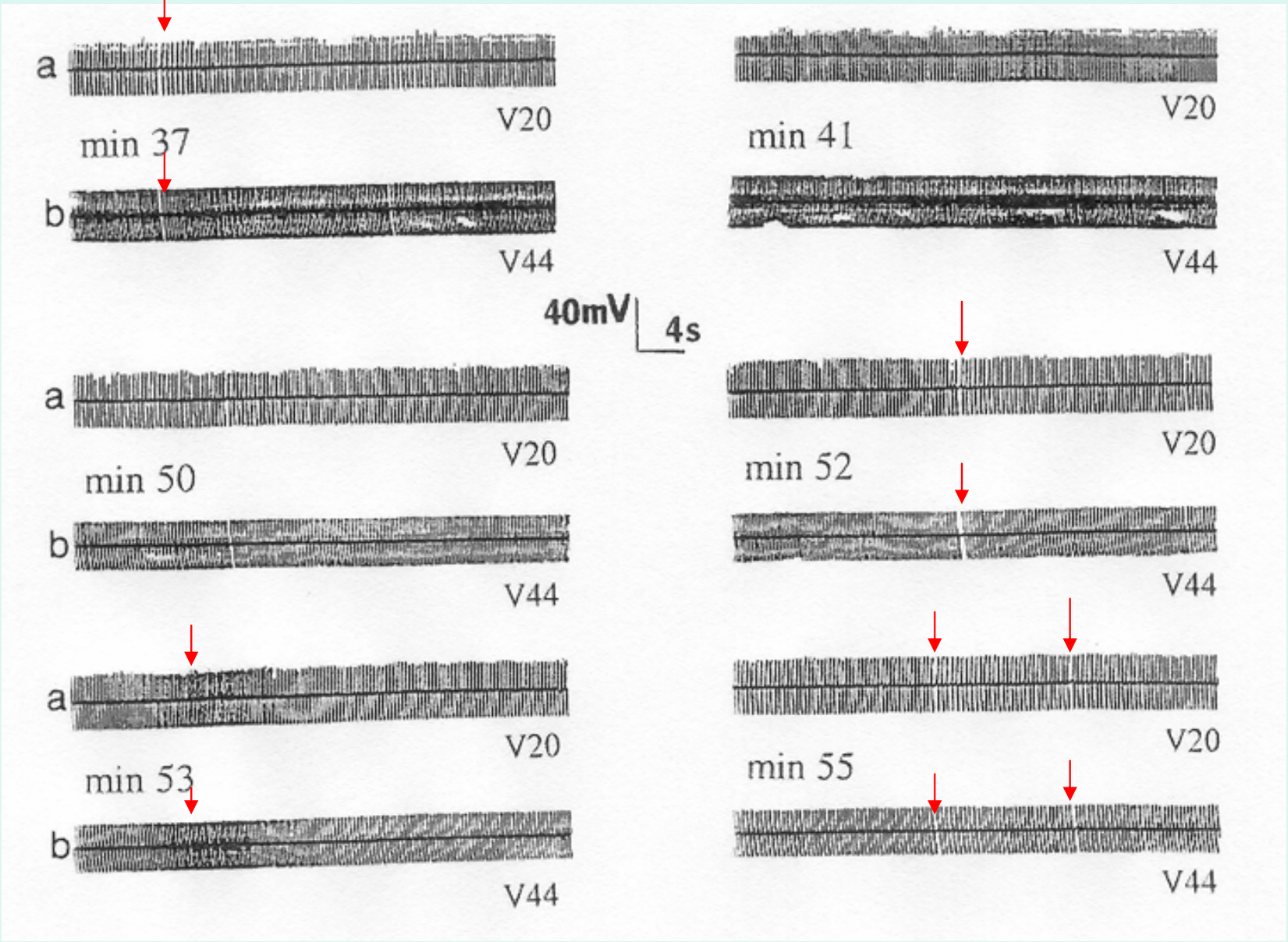

Fig.-4.- Progression of frequency synchronization (mapped neurons V20 and V44) after applying MF of 50 Hz. Note: short duration inhibition at mins 37, 50, 52 and 55 and bursting activity at min 41 and 53. On min 55 both neurons show the same frequency

v) - **decrease** of the firing frequency, *f* with the increase of the ELF-MF, **frequency ,** f_M, at constant B_0= 1mT.

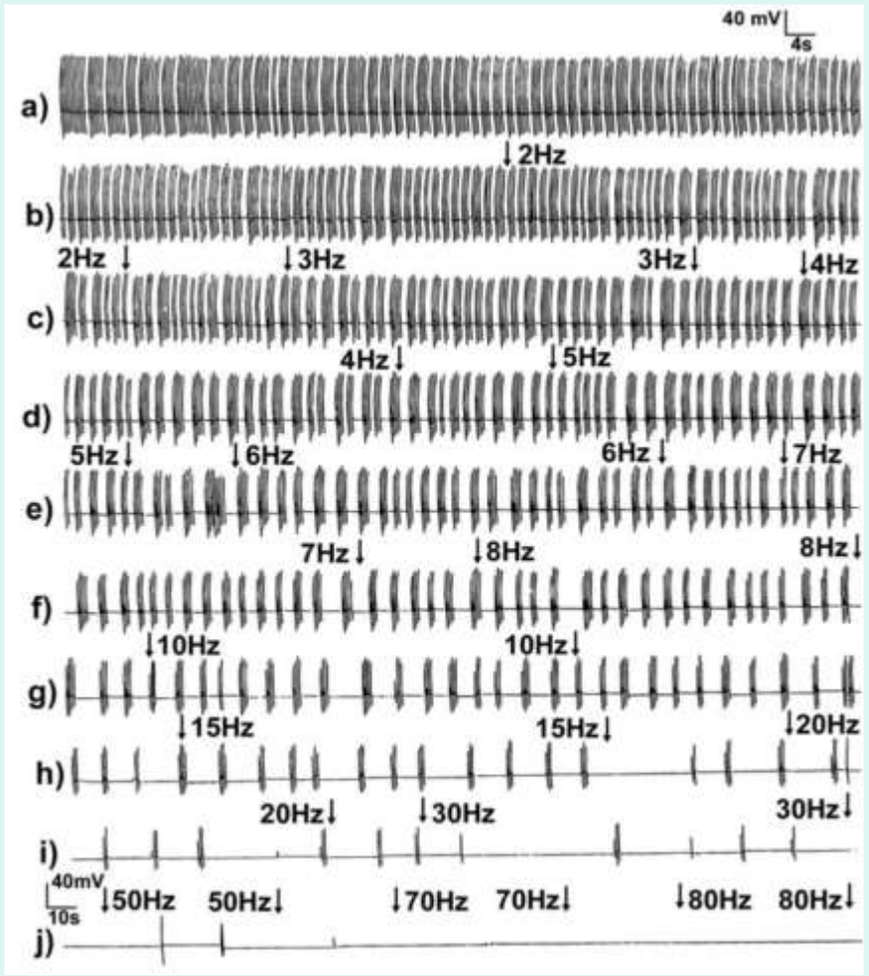

Fig.5.-

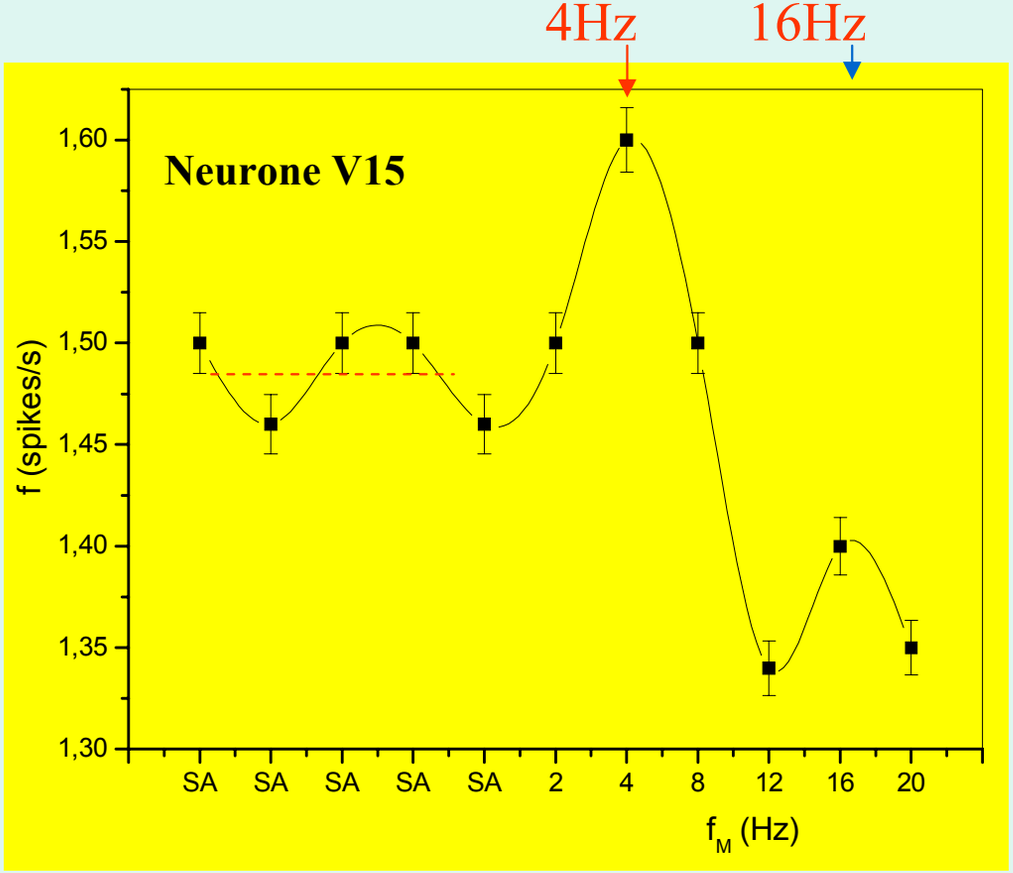

Applied 9.6 GHz microwaves carrier, modulated by ELF-MF: "resonance" at 4 Hz and 16 Hz

vi)- Some kind of **"resonance"** when both frequencies match,i.e. $f_M \cong f_0$.

Conclusion from experiments: ***firing frequency*** **is the relevant magnitude to look upon for neuron response to magnetic field, for developing a model.**

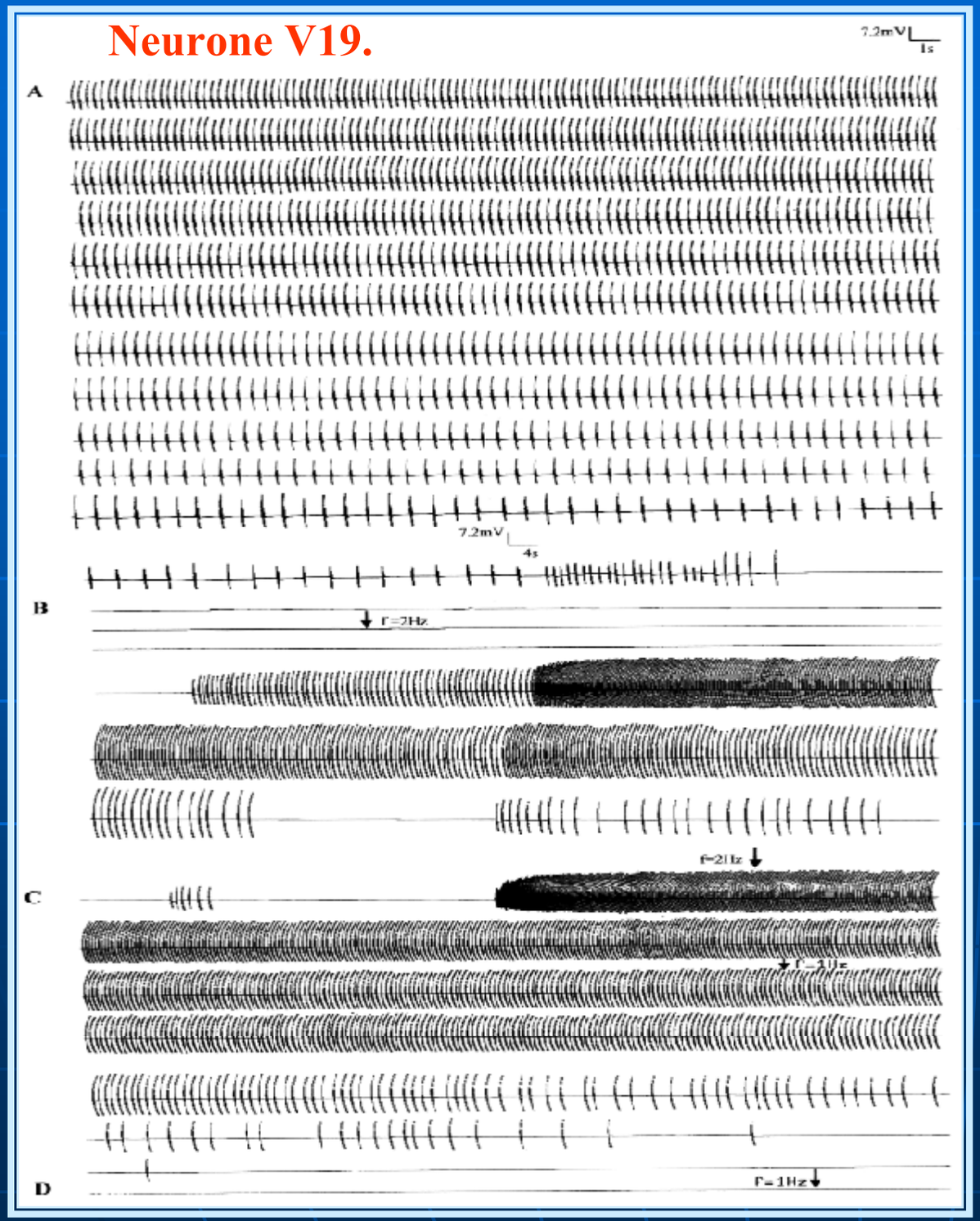

"Resonat" behaviour :

♠ A): f_0= 2.4 spikes/s, frequency and amplitude progressively decrease, being the neuron activity completely and sponta-neously inhibited after 6 min recording.

♠ B): ELF-MF of 1 mT-2 Hz, for 10 min. With 4 min delay the neuron activity is stimulated, spikes amplitude increasing.

♠ C): ELF-MF of 1 mT- 1 Hz the frequency and amplitude decrease, being the neuron completely inhibited.

♠ Experiment duration: 35 min.

Pérez-Bruzón R.N., Tesis Doctoral, Zaragoza, Spain, 2006

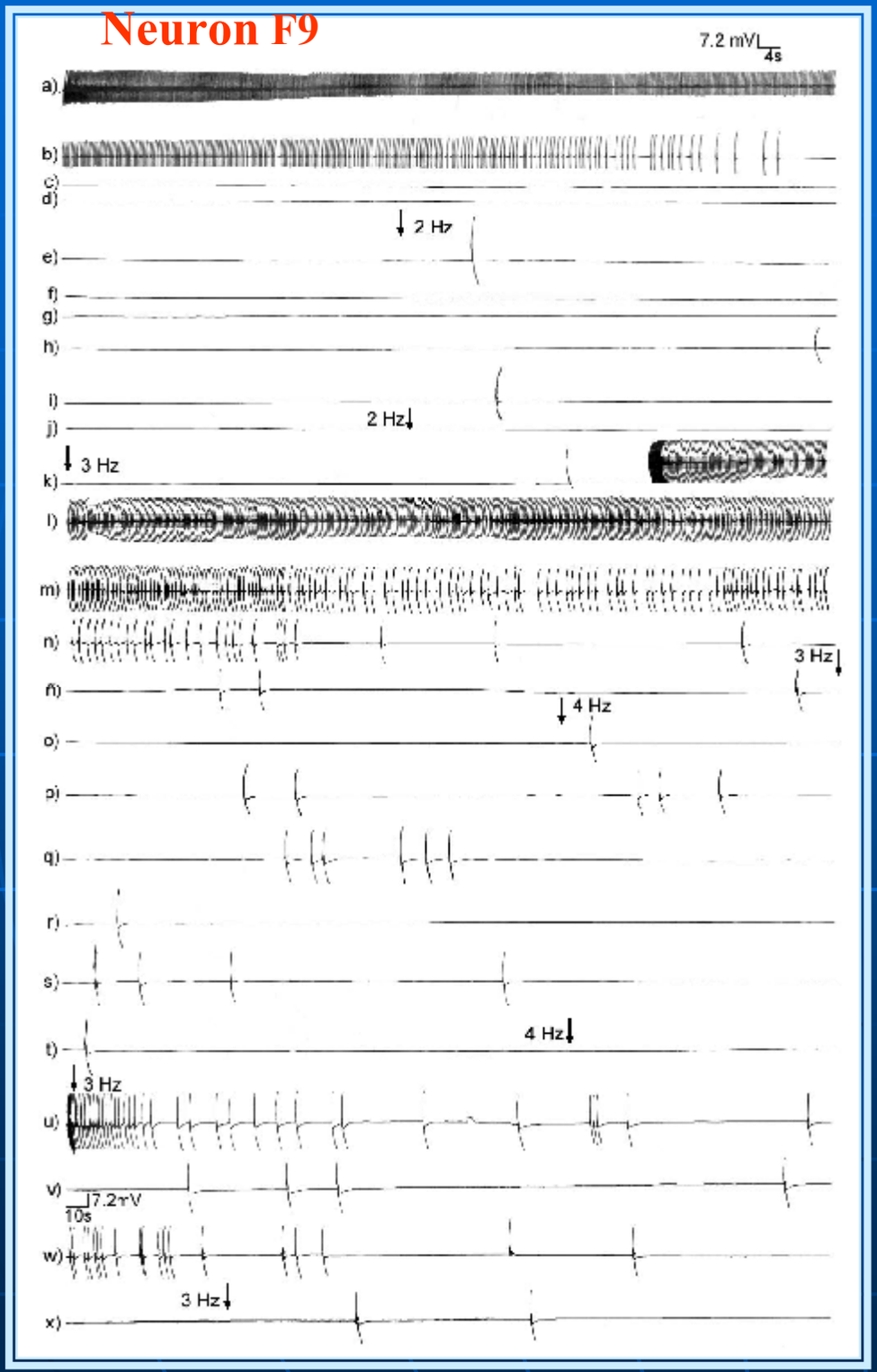

"Resonance" again:

- ♠ a-b) f_0= 3.0 s/s
- ♠ c-j) ELF-MF 1mT, f_M = 2 Hz, inhibition of neuron activity
- ♠ k-ñ) f_M = 3 Hz = f_0, stimulation!
- ♠ o-t) f_M = 4 Hz, neuron inhibited
- ♠ u-x) f_M = 3 Hz = f_0, stimulation

Experiment duration: 60 min

Pérez-Bruzón R.N., Tesis Doctoral, Zaragoza, Spain,

B. THE SD+CE MODEL.

I. MODEL BASES.

- Our *fully quantitative* **physical** model explains bioelectric activity of *single* unit neurons under **static** (SMF) and **extremely low frequency (ELF)**-magnetic fields (**B**), based upon the following assumptions:

1. Strong **anisotropy of diamagnetic susceptibility** (DS) of membrane phospholipids (PP) and Na+-K+- ATP-ase pumps.

- Magnetic susceptibility parallel to the longer PP axis, $\chi_{||}$, is different to the perpendicular one, $\chi_{\perp}$: *susceptibility anisotropy* being : $\Delta\chi = \chi_{||} - \chi_{\perp}$.

PP rod approximation in the model:

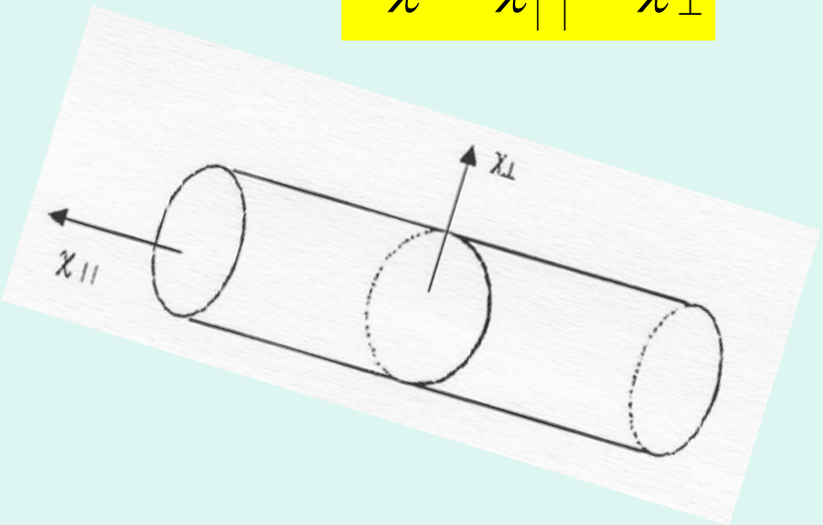

- **2.** ***Cooperative*** action of **PP**, forming large correlated **clusters** within the membrane liquid crystal: called **superdiamagnetism**. Correlation is by quadrupolar PP interaction (PP has no significant PP electric dipolar moment):

cluster formation in the **membrane** liquid crystal of ***correlated* PP** long axes $\hat{x}$ through their electric quadrupolar moments, $\tilde{Q}_i$ (tensor) interaction, of pair (i, j) *correlation function*,

$$C_Q = \langle \tilde{Q}_i Q_j \rangle - \langle Q_i \rangle \langle Q_j \rangle \propto \exp\left(-(s_j - s_i)/\xi\right)$$

by which the **PPs cooperatively rotate** out from the MF **B** axis (SD). $\langle \ldots \rangle$ is the canonical ensemble thermal average

The **correlation length**, ξ, can exceeds a single neurone, *via* the PPs of the interposed **glia membranes** between neurones, and through the gap junctions.

Quadrupolar electrical potential:

$$V_Q = (1/8\pi\varepsilon_0)\frac{\hat{r}\cdot\tilde{Q}\cdot\hat{r}}{r^3}$$

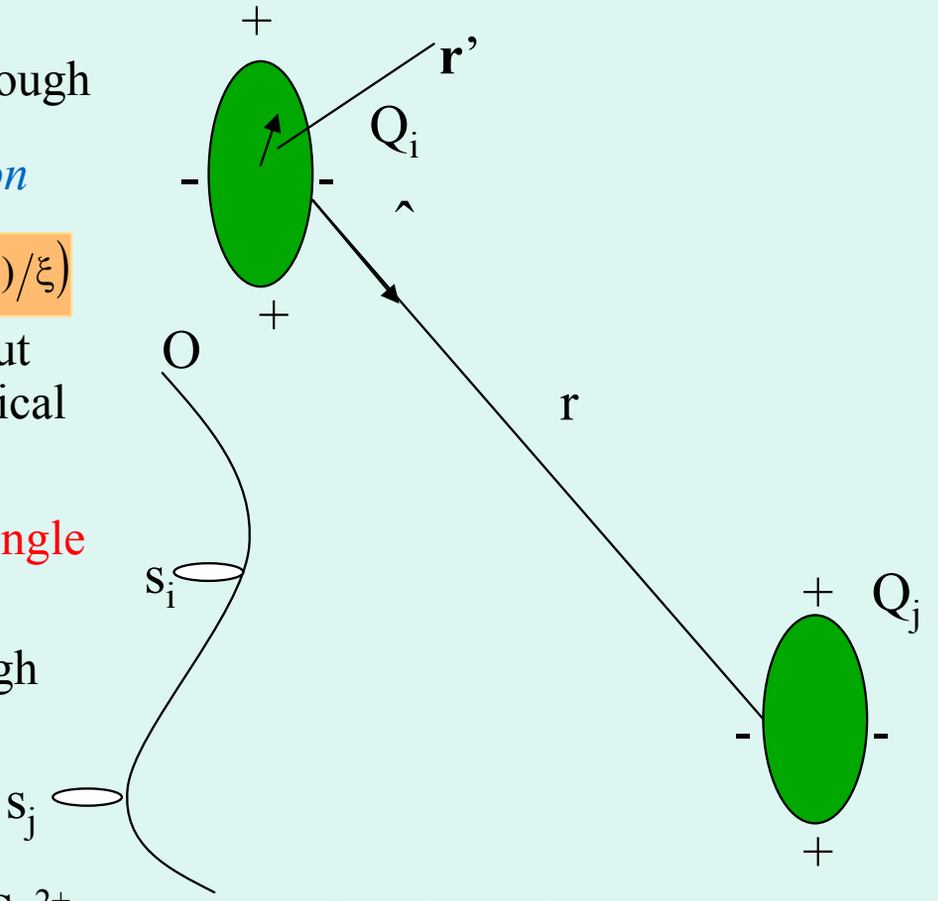

Quadrupolar moment tensor:

$$\tilde{Q} = \int r'^2 \left(3\hat{r}'\hat{r}' - \right)\rho(\ ')dV'$$

- **3**. **Coulomb explosion** and liberation of Ca^{2+} attached to PP, at *both* membrane sides. They **open Ca^{2+} -dependent-K^+-channels (CaKch).**

- * We underline: **very precise** values of parameters intervening in our model are **crucial** in order to *explain experiments*!.

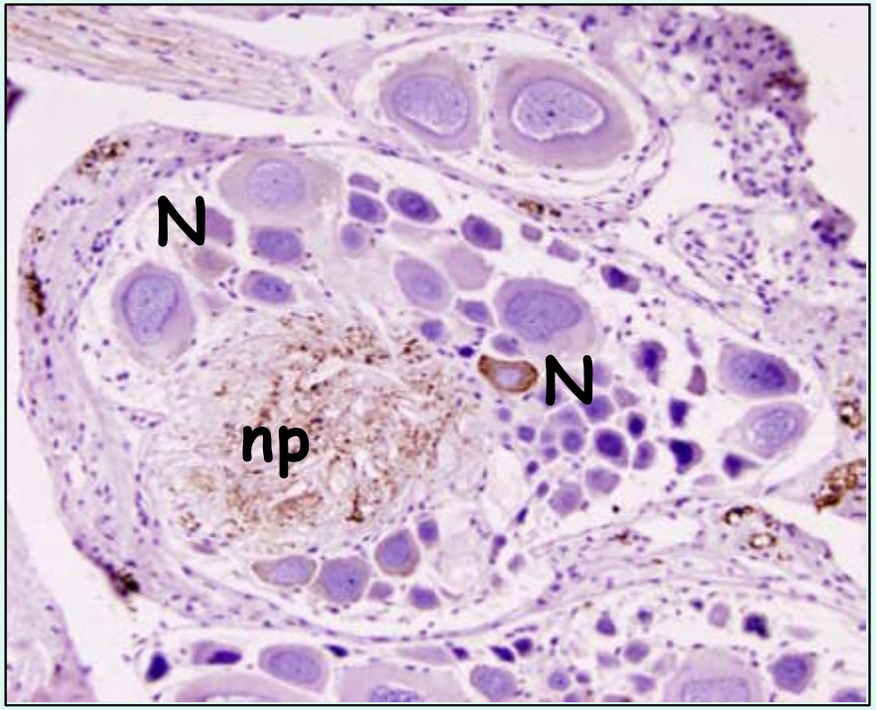

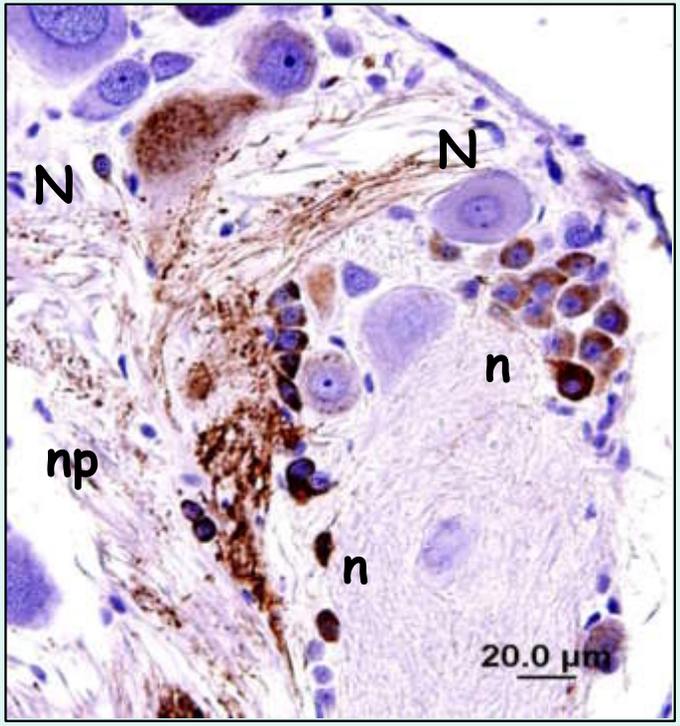

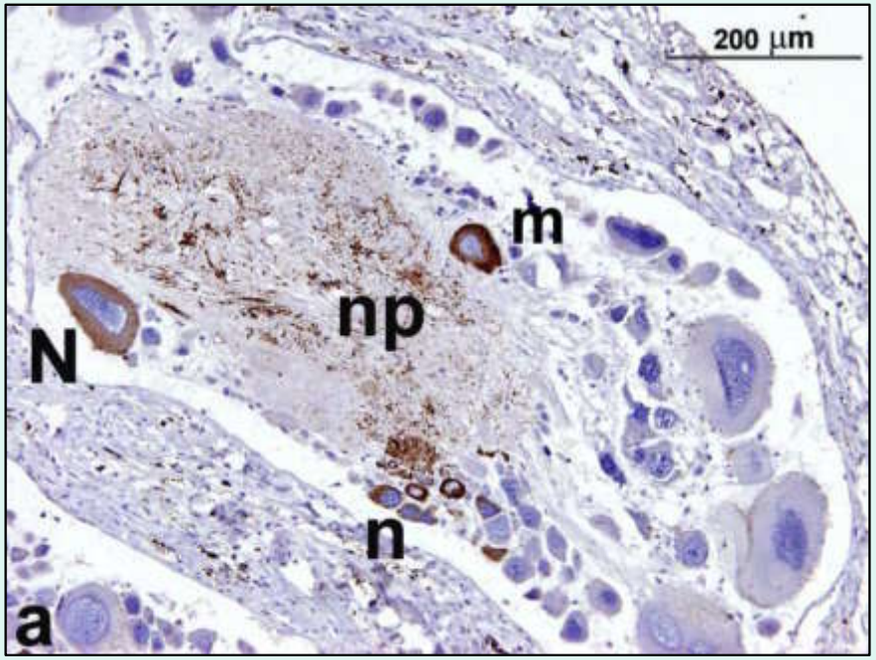

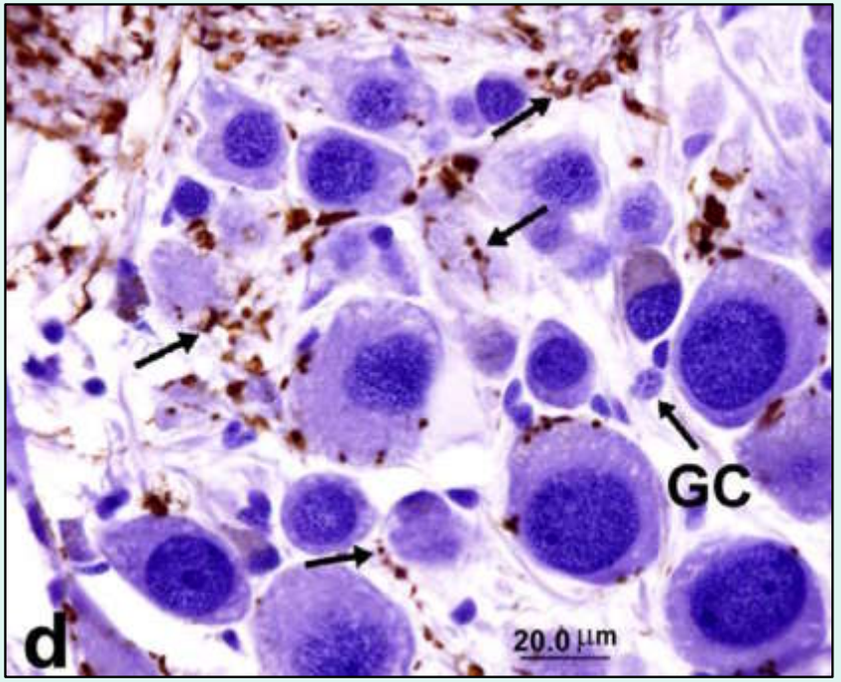

Connexin 26 expression (gap junction (-->) protein between membranes)

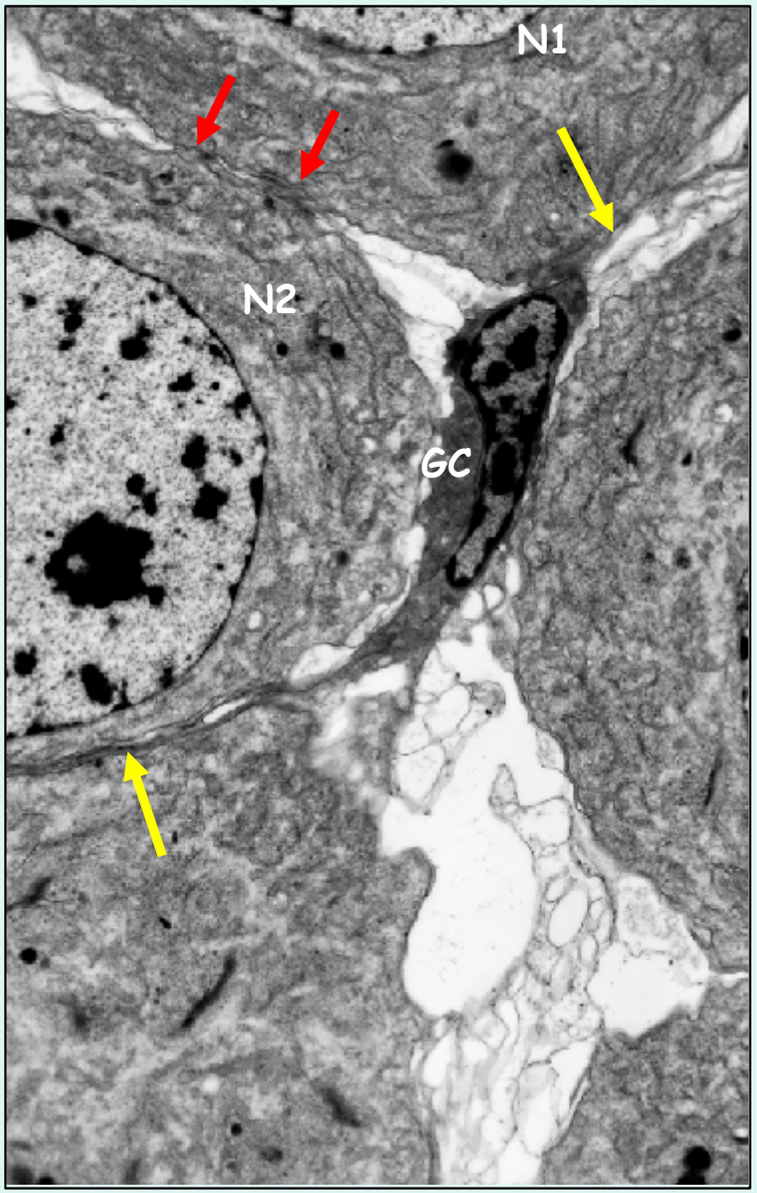

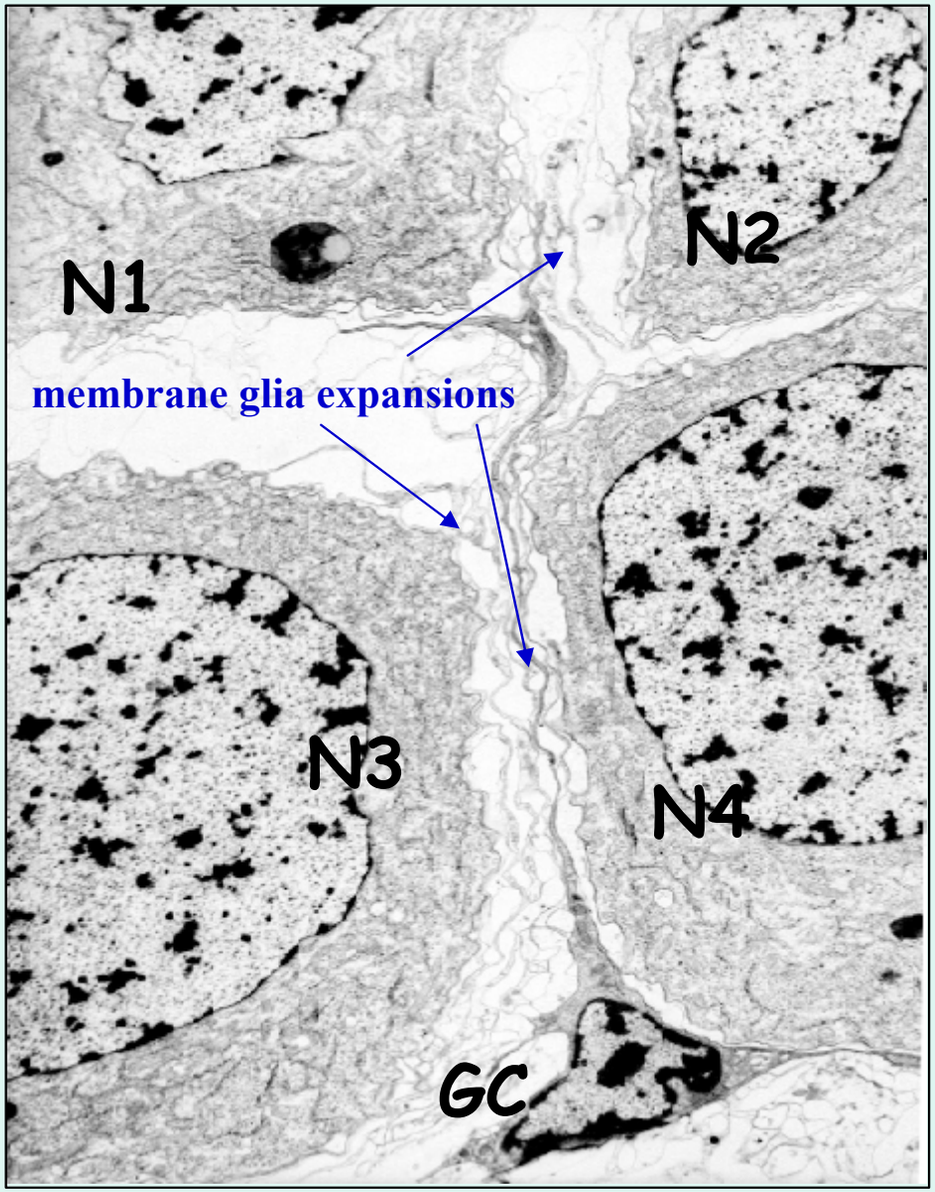

Glia cell (GC) connecting neurone membranes through gap-junctions(→)

II. MODEL DEVELOPMENT.

i) Membrane superdiamagnetism and Ca^{2+} Coulomb explosion:

* Membrane bilayer PP's , *negatively charged* (-e) at polar terminations of *phosphatidylserine* (PS) and *glycolipid* (GL), in the inner and outer halves of spherical membrane, being able to ***capture*** external and cytosolic ***Ca^{2+} ions***.

Fig.6.- Membrane average content of inner **PS molecules** is ≅ **14 %** of membrane PP's,while the **GL content** in the outer half of the bilayer is ≅ **15 % (the same)**. Bound to heads are **water solvated** Ca^{2+}, overall heads having an **effective positive charge, δ.** Interposed between the lipids are *cholesterol* molecules with **dielectric constant** ε_r = 2.21.

Crucial length! in the model are: ***l*** ≅ 60 Å and ***p*** ≅ 14 Å (obtained by Dreiding moloecular construction).

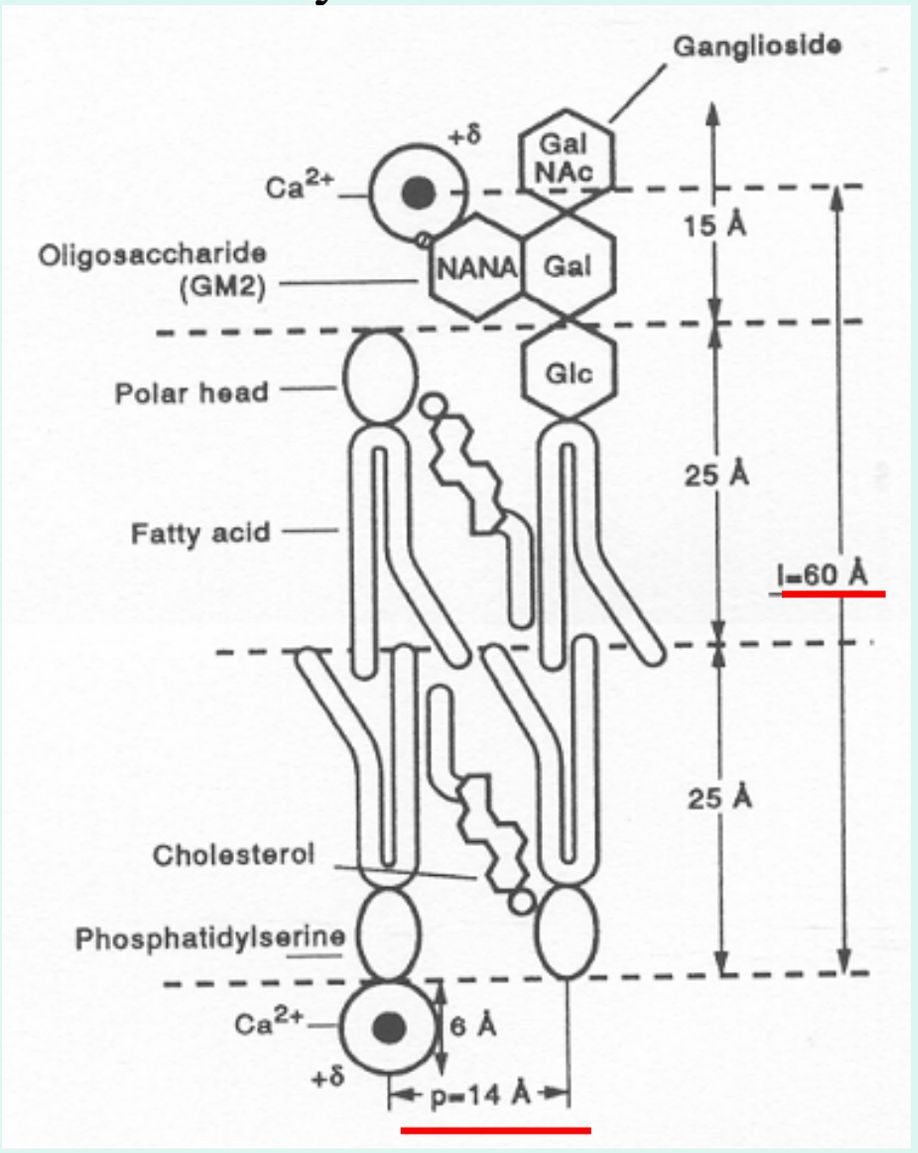

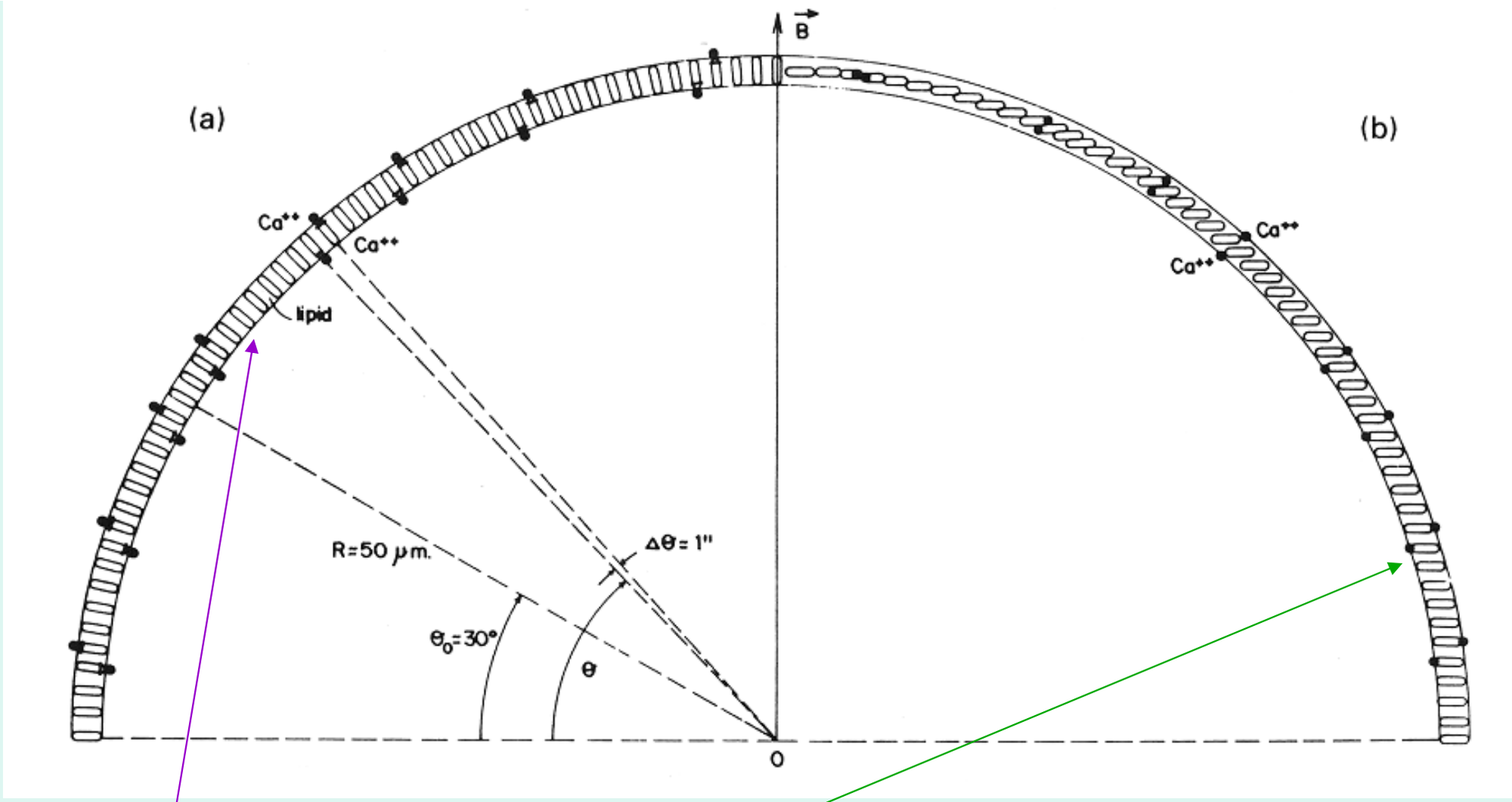

Fig.7.- a) Neuron membrane, with **nearest neighbours** PP (≅ **2%** in membrane), with Ca^{2+} ions attached. θ, polar angle of the radial PP. The calculated angle θ_0 =120º (calculated) ***below which there is not possible*** Ca^{2+} ***liberation is shown***.

b) Membrane under an applied magnetic field **B**, where diamagnetic PPs have ***fully rotated*** becoming their long axes orthogonal to **B:** then ***membrane shrinks*** (rotational dia-magnetostriction) and the Ca^{2+} charged heads **approach**.

** Because of formation of Ca^{2+} electrical images within membrane, this is substituted by bilayer with **effective charges**

$\delta^{+}_{eff} = (2\varepsilon_r/(\varepsilon_r+\varepsilon'_r))e << + e.$

where dielectric constants $\varepsilon_{r'} \cong 80$ (Ca^{2+} solvation water) and $\varepsilon_r = 2.21$ (cholesterol molecules). Strong *reduction of effective Ca^{2+} charge* down to δ^{+}_{eff} **$= 0.053\ q_{Ca}$ (**outside Debye screening length**).**

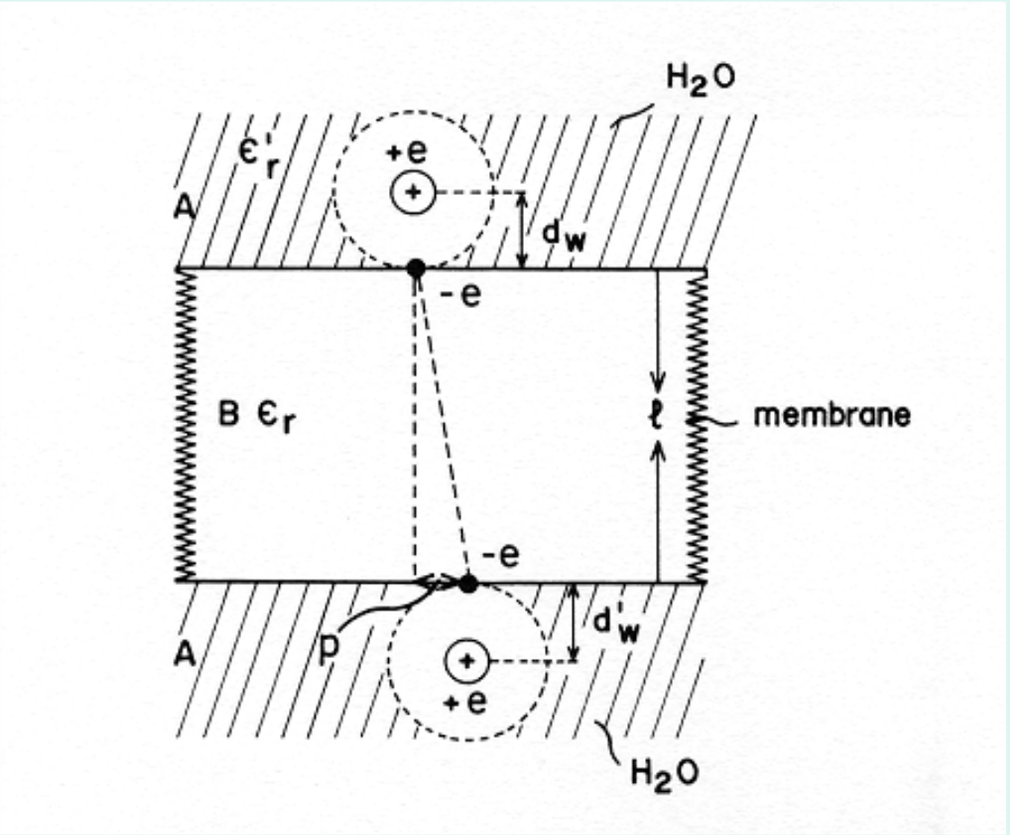

Fig.8.- Effective charge, δ^{+}_{eff}, in the Ca^{2+} ions, and polyanionic membrane surface ligands δ^{-}_{eff} charge, due to the effect of the negative electrical images formed inside membrane, which reacts on the Ca^{2+} and ligand charges as well, reducing the coulomb attraction.

Main dimensions: $d_w \cong 10$ Å , $d_w' \cong 3$ Å.

*** When SMF **B** is applied, since $\Delta\chi$ < 0 the **PP's** rotate off the **B** lines, for B > B_0 becoming **orthogonal** to **B** (Fig.7.b). For $\Delta\chi$ > 0, i.e. for **proteins** inmersed in the PP liquid crystal, rotation is the opposite one, e.g. ATTP trying to become **parallel** to **B** (Fig.9). Same should happen to Na and K protein channels, but they are firmly attached to bilayer.

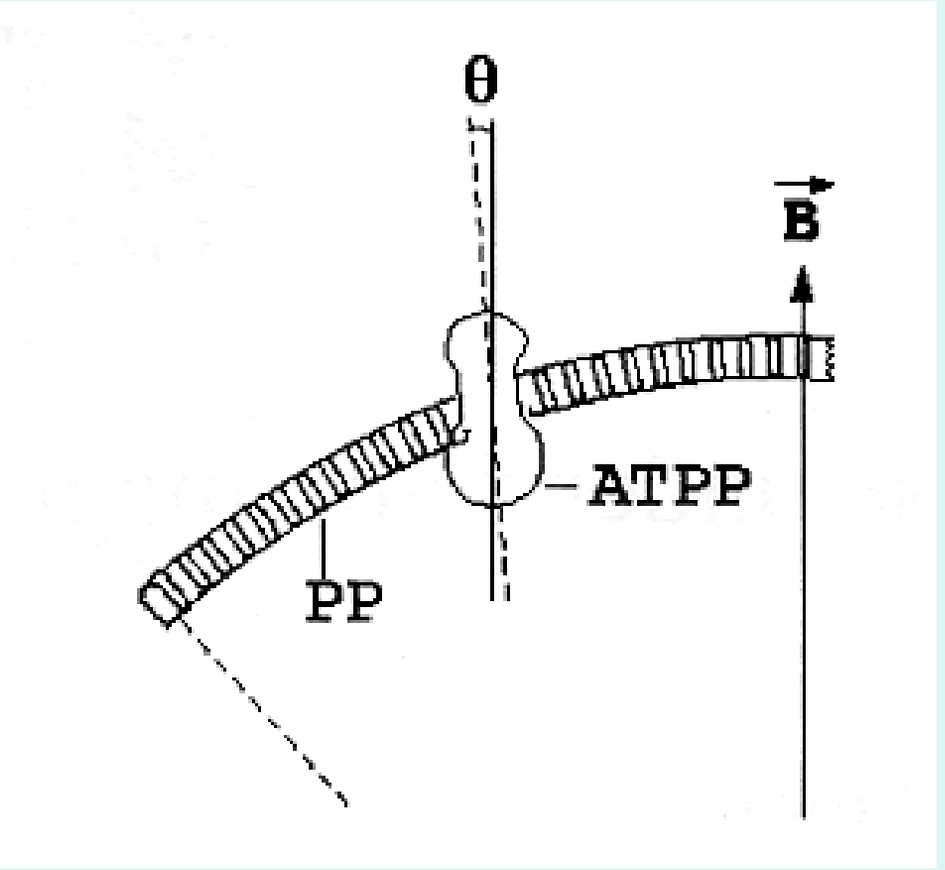

Fig.9.- PP bilayer with $3Na^+$-$2K^+$ -ATP-ase **protein pump (ATPP)**. θ , angle of ATPP axis with magnetic field **B**: protein becomes less effective in hydrolizing ATP due to rotation.

**** *If* Ca^{2+} charged PP's at *both* sides of membrane are **nearest-neighbours** (probability ≅ 2%) , there exists a ½ probability of **opposite** sense PP **rotation**, then NN **Ca^{2+} ions approaching** each other, and if Coulomb force is strong enough, ionic bond of energy, ε_b is **broken** (possible because dielectric constants ε_r(membrane) << ε'_r(solvation water).

► Ca^{2+}ions are **liberated** through simultaneous ***Coulomb explosion*** at *both sides* of membrane.

-PP ***cluster*** rotates through a *"domino"* process (correlation) and membrane thickness *shrinks* (magnetostriction-like, see Fig.7. b). This mechanism is a 0K one, important temperature effects being later included.

►In our opinion this is the ***rationale*** **to explain liberation of *static* electric charges (Ca^{2+})** by **static or quasistatic** (ELF) **magnetic fields,**

where EM energy absorption is forbidden or almost. Recall SMF or quasistatic MF Lorentz magnetic force (EF **E**≅0),

$$\mathbf{F} = q(\mathbf{v} \times \mathbf{B})$$

can not produce work upon charge for such magnetic fields:

$$L = \int q(\mathbf{v} \times \mathbf{B}).d\boldsymbol{l} = 0$$

merely since $\mathbf{v} \perp d\boldsymbol{l}$.

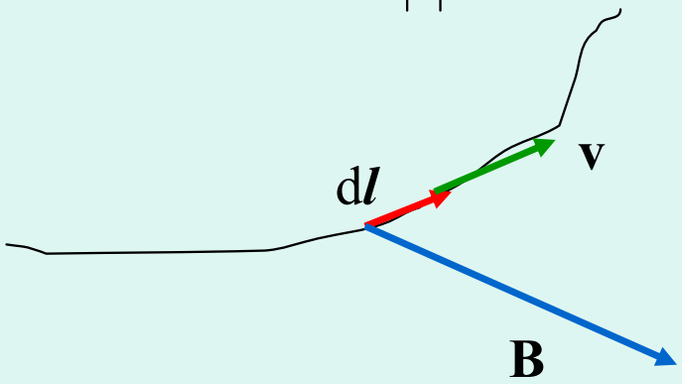

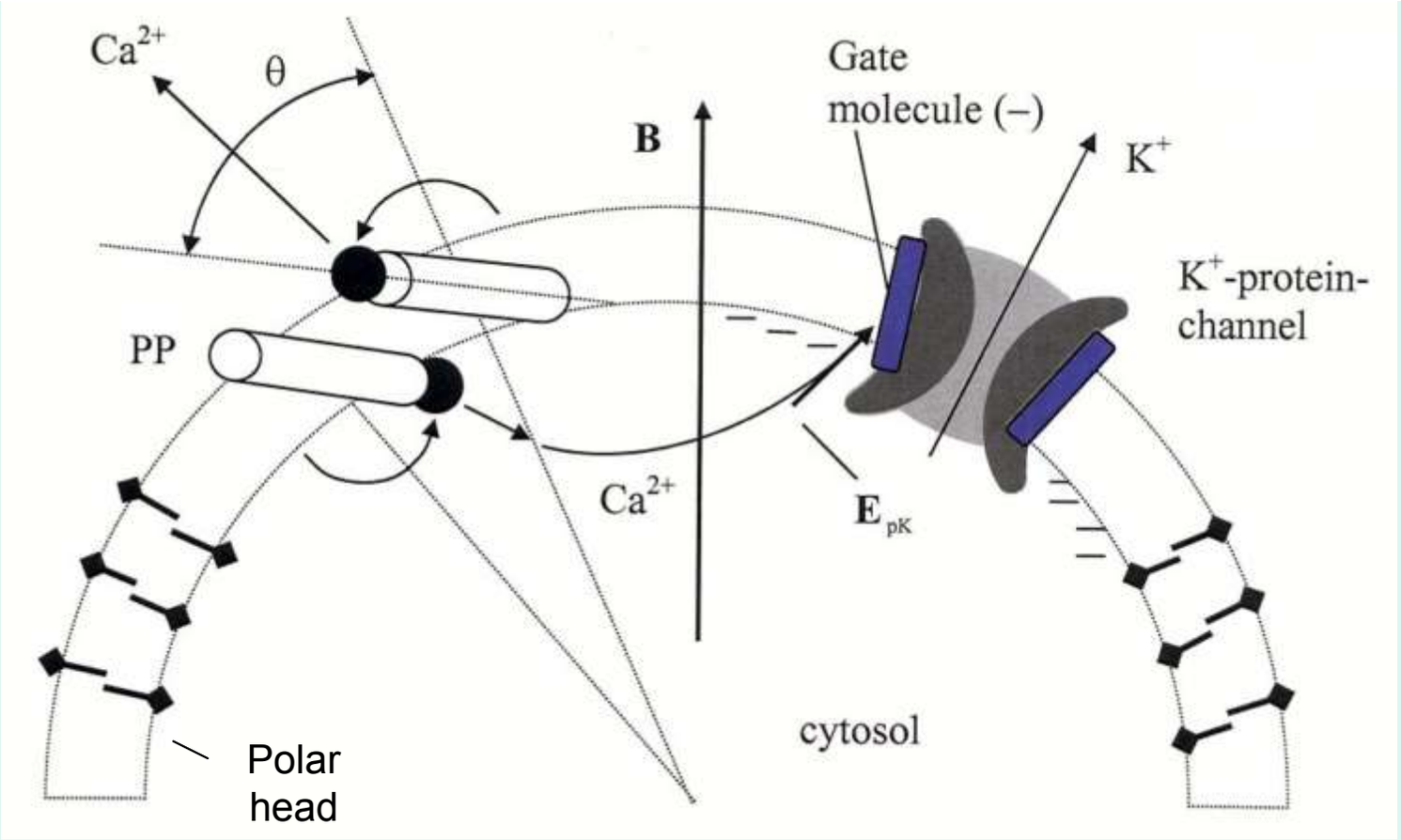

Schematic mechanisms involved in the SD+CE model:

- Two nearest-neighbour Ca^{2+}-charged phospholipids (rods) rotate under their assumed opposite **magnetic torques**, $\tau_m = \pm \mathbf{m} \times \mathbf{B}$ approaching the Ca^{2+} ions (black circles), attached to the PP negatively charged heads (lozenges). **m** is the PP magnetic moment, induced by AC MF.
- The weak ionic bindings are broken by their mutual coulomb repulsion.
- The ions become simultaneously detached from the membrane surfaces when their weak ionic bonds, of energy $\varepsilon_{coul,}$ to the heads are broken due to Ca^{2+}- Ca^{2+}- **coulomb repulsion**.
- Within the cytosol the **Ca^{2+} ions diffuse** towards the K^+-protein channels, which are opened when Ca^{2+} is captured by the "gate" molecule (calmodulin, with four anchoring points), giving rise to the outwards K^+ current (neurone hyperpolarization).

Ionic protein channels in *Helix*, observed by immunocytochemistry

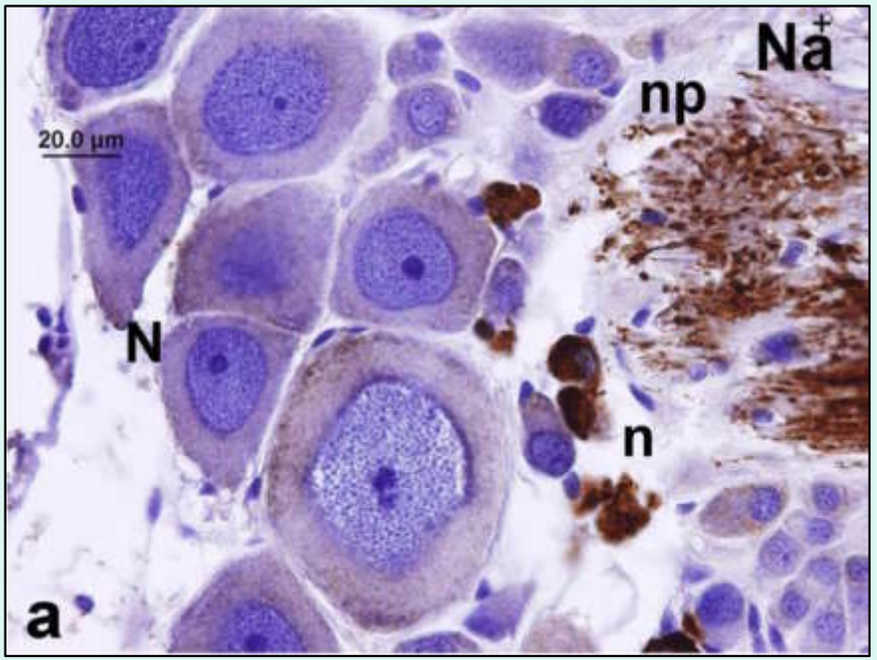

Voltage operated Na^+ channels

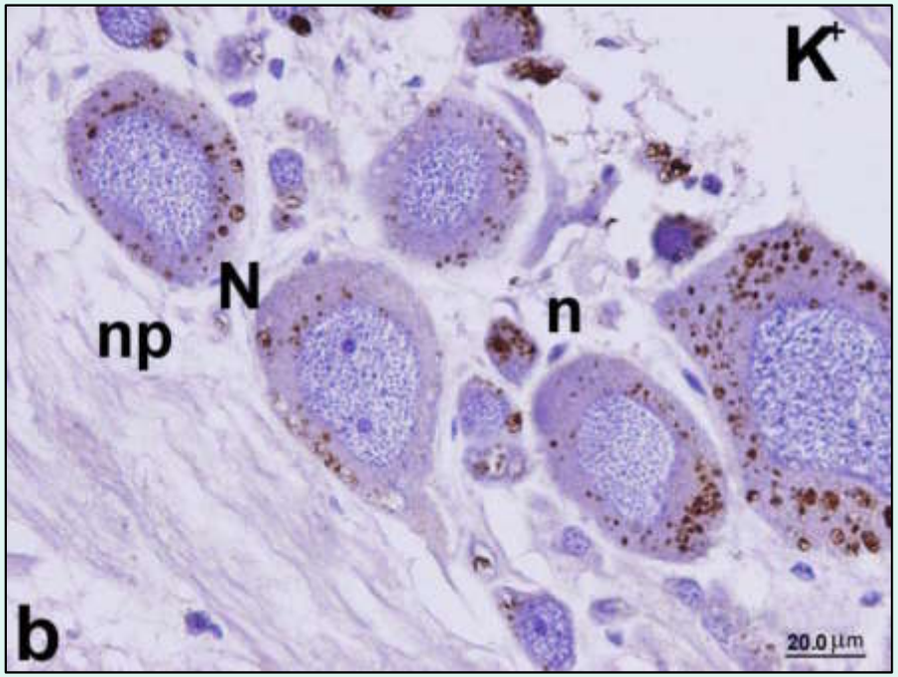

Delayed rectifier K^+ channels

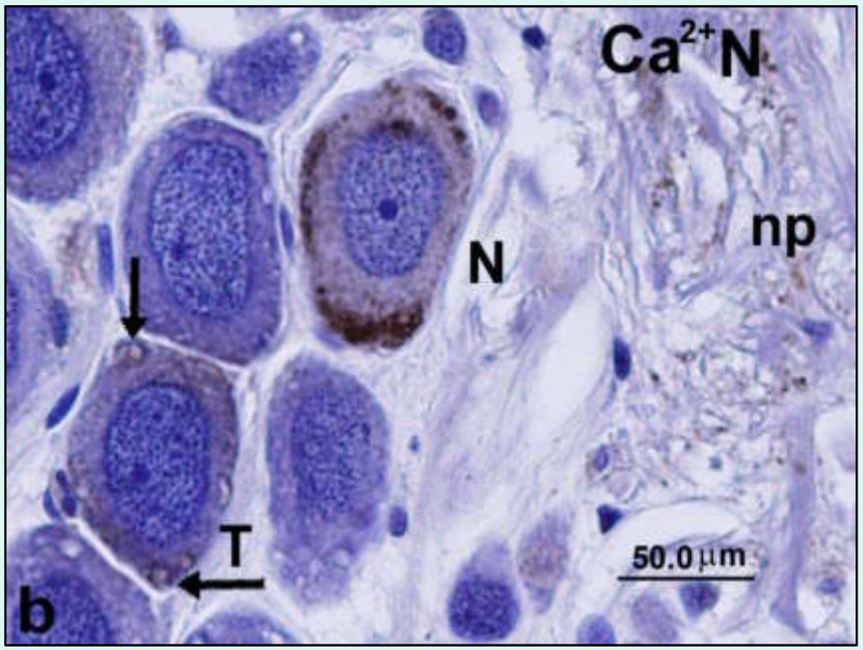

Voltage operated $Ca^{2+}N$ channels

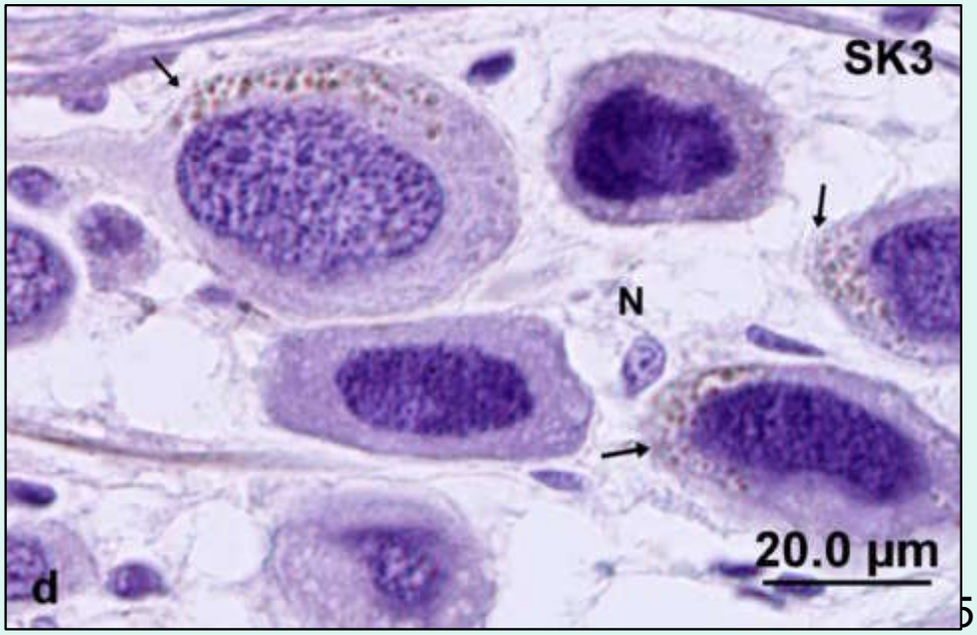

K^+ channels operated by Ca^{2+}

ii) Energetics of Ca^{2+} liberation:

* In limit position (f) when the NN Ca^{2+} charged PP have *rigidly* **fully** rotated, becoming closer than as rest positions (i), variation of Coulomb repulsion energy is,

$$(\varepsilon_f - \varepsilon_i)/\varepsilon_i = (p/l)\ \text{sen}\ \theta, \qquad [1]$$

corresponding to initial d_i and final d_f distances between the NN ***opposite*** Ca^{2+} ions (Ca^{2+}membrane attached will be stable if $\varepsilon_i < \varepsilon_b$, the binding ion energy).

Fig.10.-A) ***Intermediate*** position of charged **NN** lipid magnetic dipoles for SMF $B<B_0$,where dipoles ($+\delta^+$) have rotated angle γ under magnetic torque $\boldsymbol{\Gamma}$.

B) NN initial positions at zero field, BB' and AA' for two "active" PP's. After application of $\mathbf{B}_0$ dipoles have *fully* rotate an angle θ' .Initial Ca^{2+} distance d_i, **longer** than final d_f , and so Coulomb repulsion increases.

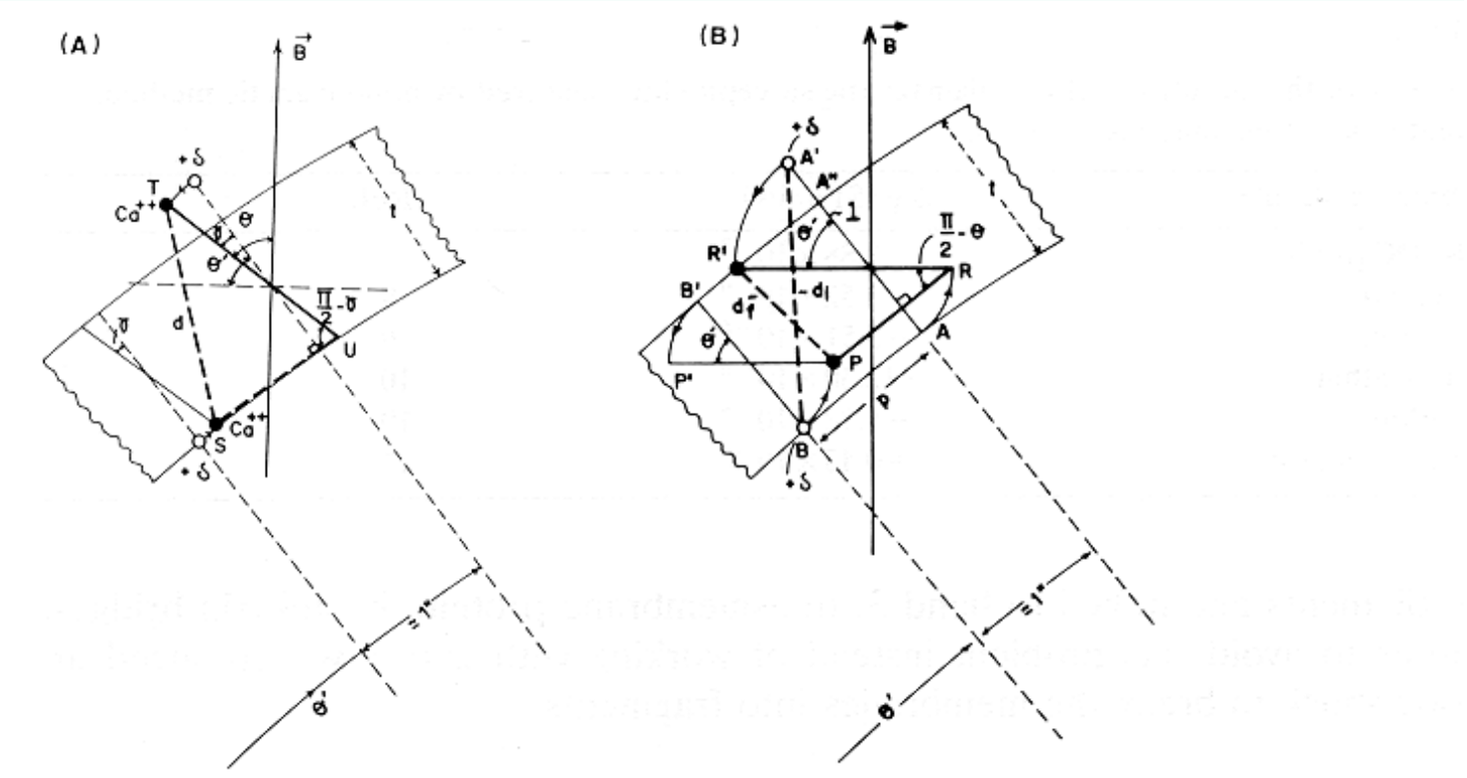

** Coulomb explosion and ion liberation happens if

$\varepsilon_f \geq \varepsilon_b$, giving the Ca^{2+} detaching condition

$\sin\theta \geq r_b\,(l/p) > 0$, with $r_b=(\varepsilon_b/\varepsilon_i) - 1$ [2]

***From [2] we deduce a *threshold* angle $\theta_0 \cong 30^o$ above which Ca^{2+} liberation *can occur* (Fig.7.b): Coulomb explosion occurs within a cap of ≅ 120º around **B**, i.e. *over a 67% of the whole membrane !*.

**** Liberation of ≈ **0.7 Ca^{2+} ions/ 100 PP** to the cytosol, with concentration increase of ≈ 2 x 10^3 $Ca^{2+}/\mu m^3$. This is **remarkable**: this concentration is ≈ *10 times greater* than the normal one (less than 100 $Ca^{2+}/\mu m^3$) and roughly of **the same order as the variation produced by the *action potential***, with the spontaneous entrance of Ca^{2+} through calcium channels, at neurone depolarization regime.

♦ ***Energies involved in Ca^{2+} liberation***:

♣ Initial *Coulomb repulsion* energy is $\varepsilon_i = (1/4\pi\varepsilon_r\varepsilon_0)(\delta^2_{eff}/d_i) \cong$ **5.2 meV**, giving an upper limit of binding energy ε_b **= 6.4 meV**, small due strong reduction of non neutralized Ca^{2+}charge (+e) by NANA and PS – e charges and membrane electrical images (down to only $\delta_{eff} = +0.053$ e).

▶ It can be argued that ε_b is smaller than *thermal fluctuation* energy $k_BT/2 \cong$ **13 meV** at 300 K for PP rotation. But we should also introduce water tension pressing upon the solvated Ca^{2+} ions, $\varepsilon_\gamma = \gamma \pi R^2_{Ca^{2+}}$ ≈ **4 meV**. Then $\varepsilon_\gamma + \varepsilon_b \cong$ **10.5 meV** roughly *contrarrests* thermal energy fluctuation. Therefore thermal dependence of bioelectric firing is expected to be important.

▶ Inner check: *radius of - charged groups* is given by

$$R^{-} = \frac{1}{4\pi\varepsilon_r'\varepsilon_0}\frac{2e^2}{\varepsilon_b} - R_{Ca^{2+}} \qquad [3]$$

where $\varepsilon'_r \cong 80$ for the solvation water and $R_{Ca^{2+}} \cong 3$ Å. Bringing ε_b to [3] one obtains $R^- = 3.5$ Å, the well *known syalic-acid (NANA) radius!*.

▶ We should underline the ***tight consistency*** *of such a "complex" calculation*!.

♣♣ Diamagnetic energy:

Magnetic energy of a *diamagnetic* molecule in an applied field of intensity **H** is

$E_M = -(1/2)\, V\mu_0 \mathbf{H}.\, \tilde{\chi}\, .\, \mathbf{H}$, [4]

Where $\tilde{\chi}$ is the susceptibility tensor, which for molecule with *cylindrical symmetry* (also ellipsoidal) has diagonal components, $\chi_\perp$ and $\chi_{||}$ along PP-axis .V is the **PP volume**. Magnetic energy becomes

$$E_M = -(1/2)\mu_0 V H^2 \left(\chi_\perp + \Delta\chi \cos^2\theta\right) \qquad [5]$$

where θ is the angle formed by **H** with OZ (cylindrical symmetry ***anisotropy energy***).

From [5]:when **$\Delta\chi < 0$**, minimum energy is reached for the molecule axis **perpendicular** to **B (phospholipid)**, and **parallel** for **$\Delta\chi > 0$ (protein channels or protein electrogenic pumps).**

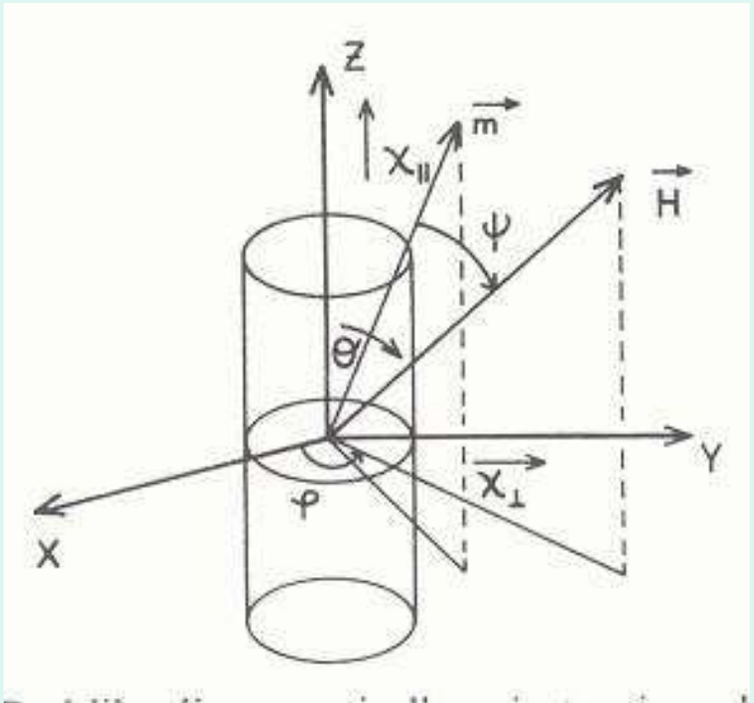

Anisotropic ($\chi_{||} \neq \chi_\perp$) PP rod, with induced magnetic moment m in applied MF **H, m = $\tilde{\chi}$ H.**

♣♣♣Torque excerpted by **B** upon the ***induced*** **magnetic moment $\mathbf{m}_d$** is

$\Gamma = -\partial E_M / \partial\theta$ and from [5] one obtains $\mathbf{m}_d$. If we calculate the *thermal average* $\langle m_d \rangle$ by Boltzmann statistics (and assume small λ parameter values, to see below) we obtain a *cluster* magnetic moment

$$M_c = \chi_r H \qquad [6]$$

where $\chi_r = \left(m_c / N_c VH \right) = \Delta\chi/2$ is the PP *rotational* susceptibility.

Predicted linearity of M_c with H agrees rather well (Fig. 11) with *measured magnetization* of red blood cell membranes, yielding $\chi_{meas.} = -(14 \pm 0.5) \times 10^{-7}$ SI (line **slope**).

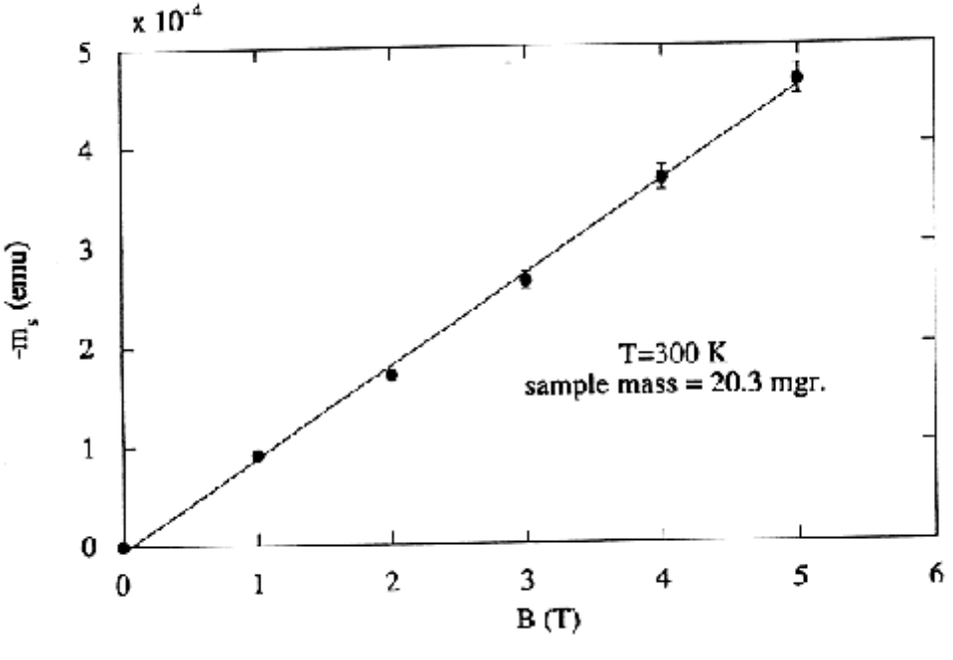

Fig.11.- Dependence of measured magnetic moment m_s with B for dried powder of red blood cell membranes (SQUID magneto-metry) . ***From the slope of m_s vs. B the magnetic susceptibility, χ_{meas} is obtained.***

♣♣♣♣ *Cluster size under SMF:*

Whole PP susceptibility is:

$$\chi_{meas} = \chi_r + \chi_\perp = \Delta\chi/2 + \chi_\perp = \chi_{||} + \chi_\perp$$

Since $|\chi_{||} + \chi_\perp| >> |\chi_\perp|$, then:

$$\chi_{meas} \cong \Delta\chi/2. \qquad [7.a]$$

► More accurately, cluster magnetic moment is:

$$m_c = (N_c V \Delta\chi/2)\, I_{er}(\lambda)\, H,$$

where $\mathbf{I_{er}(\lambda)}$ is well known **error function** and variable

$$\lambda = B\,(N_c V/2\, k_B T)^{1/2} \qquad [7.b]$$

and if we take the value $\lambda = \mathbf{0.1}$, B = 0.3 T, T = 300K, representative of our *physiological* experiments under **SMF** we obtain:

correlated PP clusters of **size** $\mathbf{N_c \approx 5 \times 10^6}$ **PP**, [8]

i.e. $\mathbf{\approx 5 \times 10^3}$ **clusters per neurone**, a large number. However for weak fields N_c becomes much larger than one single neurone.

However only N_{pq} PP's are Ca^{2+} ion charged (probability p) and are NN (probability q), conditions to liberate Ca^{2+} to cytosol (Fig.7).

♣♣♣♣♣ *Abolishing magnetic field, B_0 :*

During PP rotation (Fig. 10.A) counterbalance of magnetic and electrostatic repulsion energies reads,

$VN_c E_M = (\varepsilon_i - \varepsilon_c(\gamma)) N_p$,

where $\varepsilon_c(\gamma)$ is the Coulomb repulsion energy for a rotation angle γ (Fig.10.A) and ε_i the initial energy .

►Making the magnetic torque $\Gamma = \partial \varepsilon_M / \partial \gamma + \partial \varepsilon_{coul} / \partial \gamma = \partial \varepsilon_t / \partial \gamma = 0$, we obtain the PP equilibrium condition,

$\sin 2(\theta_B - \gamma)/\cos \gamma = B_0/B$, [9] where :

$$\mathbf{B_0 = (\mu_0 \delta^2_{eff}\, p N_p / 2V\pi\varepsilon_r\varepsilon_0 |\Delta\chi|\, N_c\, l^2)^{1/2}} \; . \qquad [10]$$

is the ***abolishing field*** (specific for each neuron), such that if $B >> B_0$, PP's will become perpendicular to **B** (Fig.10. B) and ***full*** **Ca^{2+} ions liberation** will be produced.

♥ *This is the field experimentally found where the firing frequency is abolished*, transition being rather steep (first order). **From B_0 we extract the ratio N_p/N_c.**

♣♣♣♣♣♣ We *obtain* values of N_p/N_c from B_0, and then deduce: *number of* ***"active"*** *N_p PP is ≈ 1/30 of the total number of PP within the membrane* (≈ 1.6 x 10^{11} is PP number for a standard neuron of ≈100 μm diameter).

iii) Magnetic field dependence of neurone firing frequency.

Model main goal: calculate **field dependence of the neuron firing frequency**. In Fig. 13 we schematize the *dynamic* Peierls energy barrier,

$$\Delta E_c(\theta) = -(N_c \varepsilon_m + N_{nn} \varepsilon_{coul})$$

to be overcome by the complex Ca^{2+}-PP in going from the "initial" $\theta_B = \theta_0$ position to a "final" θ'_B one under applied SMF or ELF **B** ($\gamma = \theta'_B - \theta_0$).

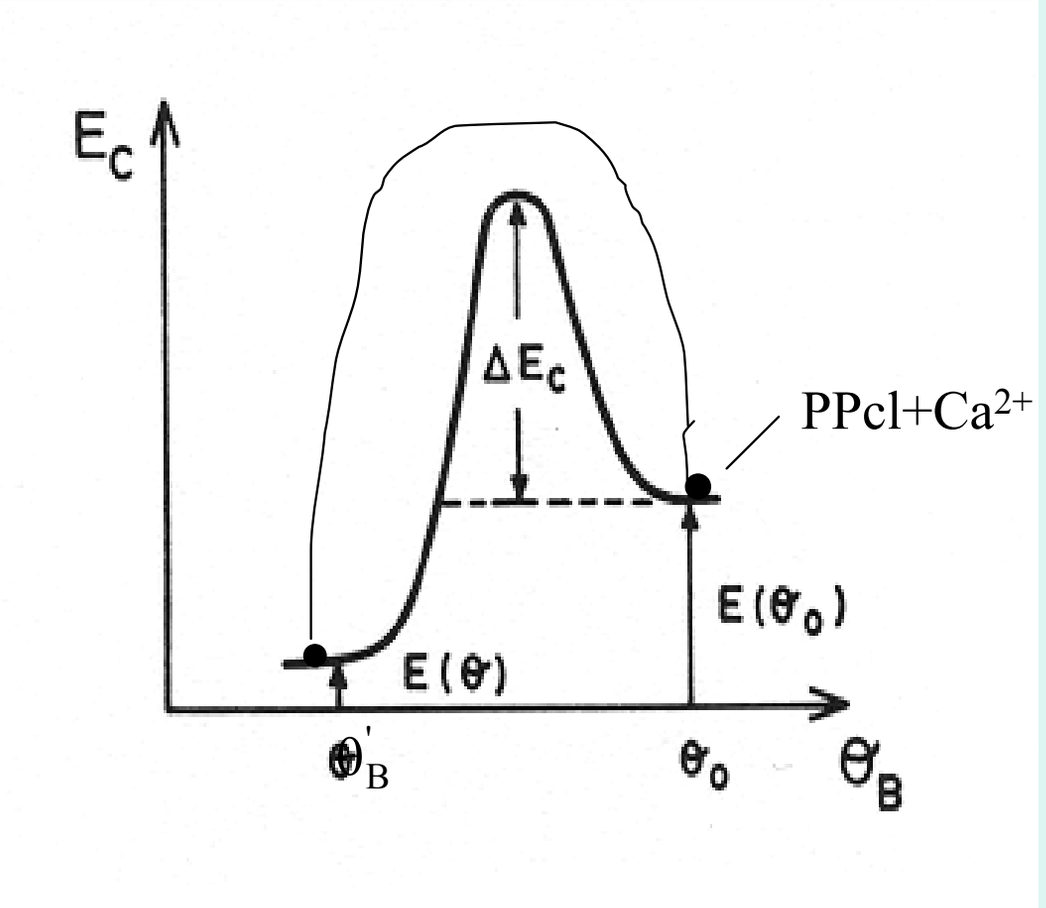

Figure 13.- Ca^{2+}-PP cluster energy against the angle, θ, formed by the PP cluster molecules with the applied field **B**. $\varepsilon(\theta_0)$ and $\varepsilon(\theta)$ are the cluster energies at the "initial" state ($\theta = \theta_0$) and "final" cluster rotation angle θ. An **energy barrier ΔE_c** has to be overcome, **which changes its value with θ_0**. θ_B is the generic angle of the PP dipole with **B**. PP nanoscopic quantum tunnelling could be also possible, although being at low T it is not observed.

♠ Now in more detail *total* Ca^{2+} -PP complex relevant energy is

$$\varepsilon(\theta_B) = \varepsilon_b + \varepsilon_{coul.}(\gamma) - \frac{B^2 V}{2\mu_0}\left(\chi_\perp + \Delta\chi \cos^2 \theta_B\right) \qquad [11]$$

►Ca^{2+} ion will be *released* when $\varepsilon(\theta_B) = \varepsilon_b$ (binding energy) , so that the dynamical ***energy barrier*** to be overcome by a PP *cluster* is

$$\Delta E_c = N_c V\left(B^2/2\mu_0\right)\left(\chi_\perp + \Delta\chi \cos^2 \theta_0\right) - N_p \varepsilon_c(0) \qquad [12]$$

where recall: N_c *is the number of PP's in the cluster and* N_p *the "active" ones* (ΔE_c *varies along the membrane, since* θ_0 *does so*).

♠♠ At **temperature T** the *Ca^{2+} ions number released* per cluster at θ_0 position, according to Boltzmann statistics is

$$N^{c}_{Ca^{2+}}\left(\vartheta_0\right) = N_p \exp\left[-\Delta E_c(\theta_0)/k_B T\right] \qquad [13]$$

and integration of equation [13] over θ_0 (active membrane), to consider all membrane clusters, yields a total number of **Ca^{2+} ions liberation:**

$$N_{Ca^{2+}} = N_P I(\lambda) = N_p \exp\left[-\left(\frac{N_c V \chi_\perp}{2\mu_0} B^2 - N_p \varepsilon_c(0)\right) \Big/ k_B T\right] \qquad [14]$$

where $I(\lambda) = (4\pi/\lambda)\, I_{er}(\lambda)$, the latter being the error-function.

♠♠♠ Experimentally firing frequency *f* decreases with increasing of B. This is interpreted as a result of :

the *membrane hyperpolarization produced by the efflux of* K^+ *ions through* Ca^{2+}*-activated-*K^+*-channels* ⟶ ***the decrease of positive voltage membrane (from resting potential), so decreasing the probability of firing and therefore the ansat for bioelectric frequency is :***

$$f = C / N_{Ca2+} ,$$ ***main model equation.*** [15]

➔This is theoretically justified by chemistry *mass action law*,

$$[P_{ch}] = \kappa [Ca^{2+} - P_{ch}] / [Ca^{2+}] ,$$ 16]

where $[P_{ch}]$, $[Ca^{2+}]$ and $[Ca^{2+} - Pch]$, respectively are *concentrations* of : **Pch , *open* protein channel (final binder),** cytosol Ca^{2+}, and $Ca^{2} - P_{ch}$, of the complex. κ`(B,T), the chemical kinetics constant. Therefore,

$$f = C[P_{ch}] = C / [Ca^{2+}] \quad \text{,with} \quad C = \kappa(B,T)[Ca^{2+} - Pch]$$

♠♠♠♠ Series expansion of $I_{er}(\lambda)$ gives for small λ or ***small B***, the **main expression in the model**

$$f(B) = f(0)\exp(-\alpha B^2) \qquad [17a]$$

with:

$$\alpha \equiv \left[-\frac{N_c |\chi_\perp| V}{2\mu_0 k_B T} \right] \qquad [17.b]$$

where $f(0)$ is the *spontaneous* frequency
Note that for 0.7 T, $\lambda = 0.045 << 4$, the latter value needed for $\pi/2$, or PP full rotation.

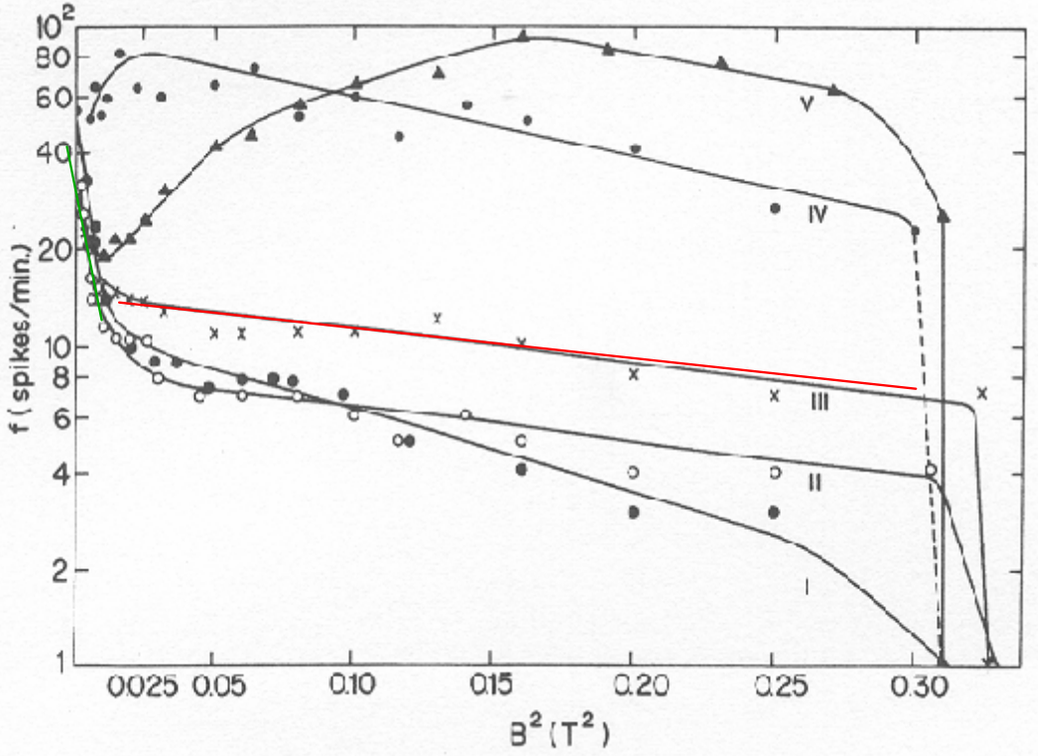

♠♠♠♠♠ Comparison of the **theoretical prediction** [17] with *experimental results* shows that prediction is ***very well followed*** : **large region of lineal variation with B^2 is fulfilled**. Larger slope (≅ 80) at weak fields B indicates much larger N_c clusters: $N_c \cong 4x10^8$.

■Slopes , α, are close for neurones II-V: good regularity: similar N_c values.

■■ Two SMF regimes: slopes **red** and **green**: change at ≅ 0.1 T. This is interpreted as the "fracture" of the low-B cluster under stronger B, due opposite magnetic torques in PP missalignment defect:

The experimentally measurable **slope**,

$$\alpha = N_c \left|\chi_\perp\right| V / 2\mu_0 k_B T \qquad [18]$$

provides ***strong support*** *to our model* ***as follows***:

- If we take $N_c \cong 5 \times 10^6$ PP/clusters as obtained from λ parameter and *independent* **magnetization measurement** on erythrocyte membranes, we **obtain the values for** $\left|\chi_\perp\right|$ **shown in Table**, (reasonably close for *all* tested neurons).

Neuron	B_0(T)	N_p/N_c (x 10^{-5})	$\lvert\chi_\perp\rvert$ (x 10^{-7})
I	0.558	1.4	0.87
II	0.575	1.5	0.38
III	0.570	1.5	0.38
IV	(0.550)	1.4	0.66
V	0.566	1.4	0.50

Again:

* ratio N_p/N_c ,**obtained from** ***abolishing field*** **B_0.**

** $\left|\chi_\perp\right|$, **obtained from** ***field dependence of firing frequency f (B).***
(from the **electro-physiological experiments !**)

♦ ♦From our *independently* **measured susceptibility** we obtain (in SI units) $\Delta\chi = \chi_{\|} - \chi_{\perp} \cong 2\chi_{meas} = -(28 \pm 1) \times 10^{-7}$, and the average **physiologically measured** $\chi_{\perp} = -0.56 \times 10^{-7}$, then: $|\chi_{\|}| = 28.56 \times 10^{-7} >> |\chi_{\perp}|$ **as we expect for a rod-like molecule**, of $l >> d$ (**not measurable** by SQUID **magnetometry, unless growing of PP single crystal**!)

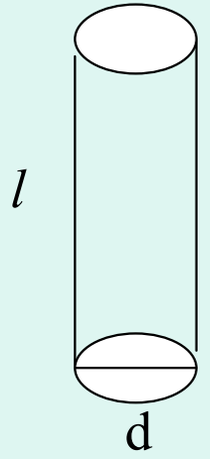

<u>This remarkable accord gives strong support to the model!.</u>

Spontaneous frequency temperature,T dependence:

★ Such a T dependence is **in disagreement with eq.[17]**

(see Fig.14).

The reason is that this neurone belong to the 26% of studied ones where ***f increases* with increasing B_{eff}** (1). The responsible mechanism is that the by MF detached Ca^{2+} ions depolarize the membrane, through their electric potential, ΔV_{ca},(*) cytosol becoming more positive, so opening Na^+ and/or Ca^{2+} channels operated by voltage, and so

$$f \propto [Ca^{2+}] = f_0 \exp(+\alpha B_{eff}^2)$$

★ ★ ***In vitro*** observation of two *phase transitions* in membrane liquid crystal at $T_{p1} \approx 33$ ºC and $T_{p2} \approx 37$ ºC : rapid *f* increase, indicative of PP perhaps critical fluctuations.

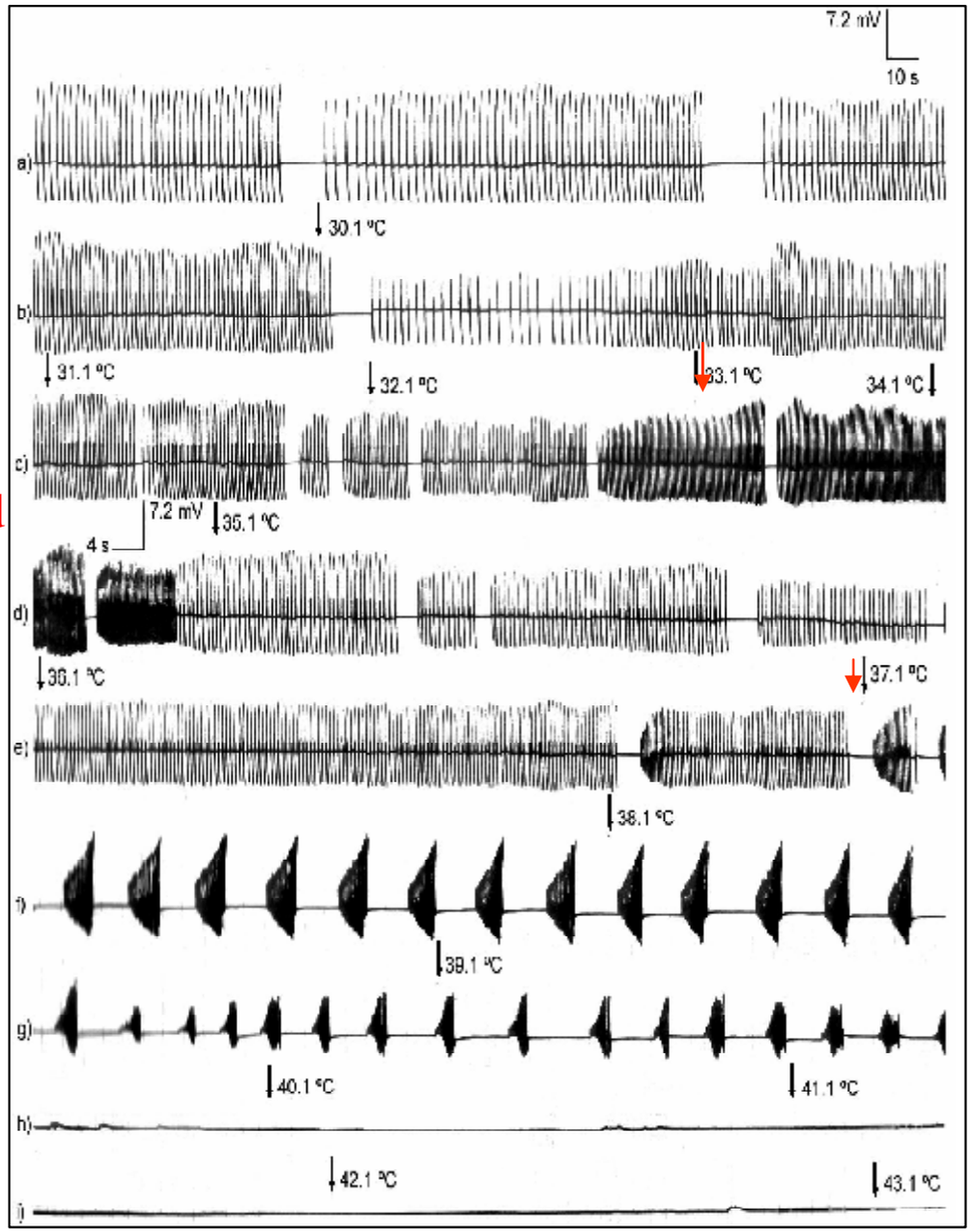

Fig.14.-

*) For a spherical neurone of membrane thickness δ,

$$\Delta V_{Ca} \cong \left(R\,\delta\, q^{eff}_{Ca^{2+}} / 3\,\epsilon_r \epsilon_0\right)[Ca^{2+}]$$

across membrane (of radius R).

(1) **Azanza M.J., and del Moral A. Prog. Neurobiol. 44: 517-601, 1994.**

v) Depolarization voltage (d.v.) decrease under magnetic fields.

- Decrease (Fig.3) is due to **ATPP protein pumps** reorientation in **B**, to become with *longer axes* parallel to **B**, off natural radial direction (Fig.9).

●● ATPP solved in PP liquid crystal and due to rotation, protein becomes ***more "immersed*** " in the PP liquid crystal: **active surface *decreases*** and **pump losses efficiency**.

●●●Therefore Na^+ cytosolic concentration increases, in turn decreasing transmembrane Na^+ concentration gradient (Nernst) and hence **depolarization voltage (d.v.) decreases**.

●●●● Pumping takes off +e net charge leaving inner membrane face negatively charged. The decrease under MF in charge transferred by a protein channel *cluster* is

$$\Delta q_d^c\ (B) \approx N_a e \exp(-N_a E_M / k_B T)$$

, $N_a E_M$, is ATP-ase magnetic cluster energy, N_a the ATPP's/cluster.

●●●●● Summing up over all N_{pc} ATPP clusters in membrane and use of Gauss theorem to evaluate the electric field within membrane due to the trapped charge Δq_d^c (B), the *decrease* in voltage across membrane is given by

$$\mathbf{\Delta V_d(B) \cong - (4\pi/N_{pc})\ \varepsilon_{fb} \exp(+ \alpha B^2)},$$

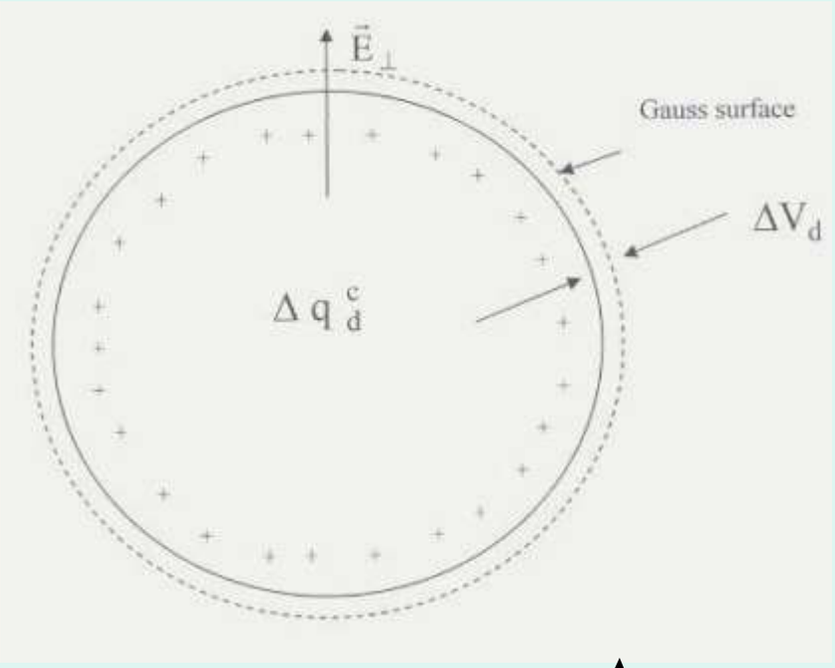

► ΔV_d is calculated from + Δq_d^c using Gauss theorem:

$$\oint \mathbf{E}.d\mathbf{s} = \Delta q_d^c / \varepsilon_r$$

for obtaining **E** across membrane.

$\varepsilon_{fb} \cong 7$ mV is the electrogenic pump e.m.f., V_p is the ATPP volume and ATPP $\Delta\chi \cong + 0.43 \times 10^{-6}$.

♦ Plots of observed **decrease** in depolarization voltage against B_0^2 for four neurons, follow well the prediction:

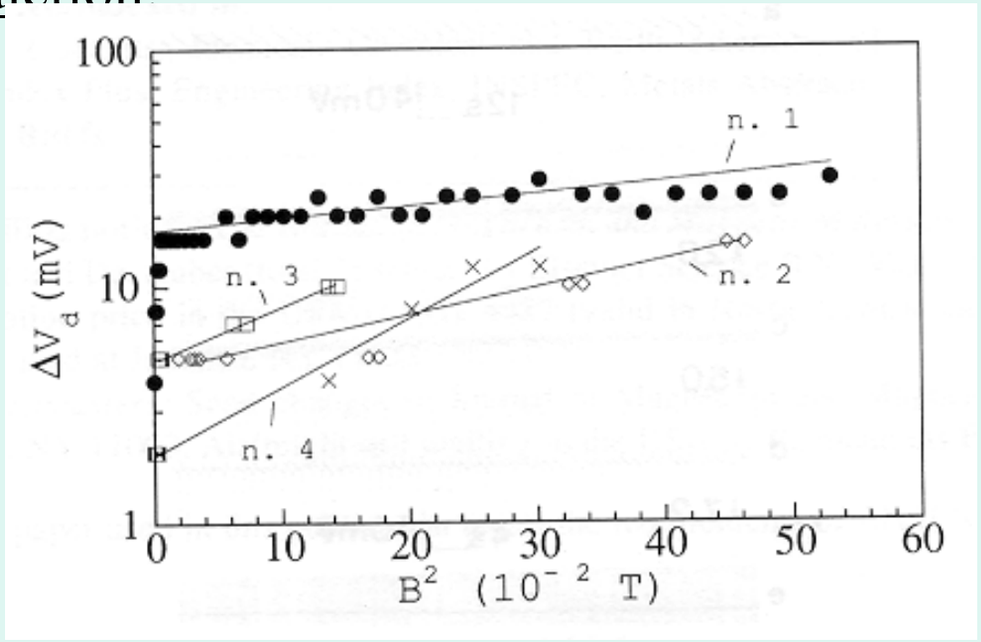

Fig.15.- Semilog plot of log. depolarization voltage ***decrease*** versus B_0^2 for four neurons.

- From α slope we obtain **N_a = (0.15-5.9) x 10^4** ($\approx 1/10^2$ - $1/10^3$ N_c , reasonable).

Note : number N_a x N_{pc} per neuron (N_{pc} between 5- 47) of *active* ATPP's per membrane is well correlated with measured neuron radius (≈ 100 μm). However hindrance of ATPP rotation by plasma cytoskeleton could be involved, reducing easyness of rotation process.

vi) Extremely low frequency (ELF) magnetic fields.

- For applied ELF-MF neurons respond more strongly when the applied frequencies, f_M *in the range of the spontaneous neuron firing frequencies*, $f(0)$, to be considered in Part II in more detail.

Applied ELF field is $B = B_0 \cos \omega_M t$, and substitution in [17] gives

$f(B) = f(0) \exp\{-\alpha B^2_0 \cos^2 \omega_M t\}$.

- For small applied fields, $\alpha B_0^2 < 0.02$, it allows to expand the exponential up to B^2, and if f_M is $\geq$ 1Hz, **the order of $f(0)$,** we can take the B^2 time average (**effective field** $B_{eff} = B_0/\sqrt{2}$) and obtain

$$f(B_0) \cong f(0)\ \{1-\alpha B^2_0/2\}\ , \qquad [20]$$

Excellent agreement with observed decrease of $f(B_0)$ for a couple of neurons V20-44 for f_M = 50 Hz :

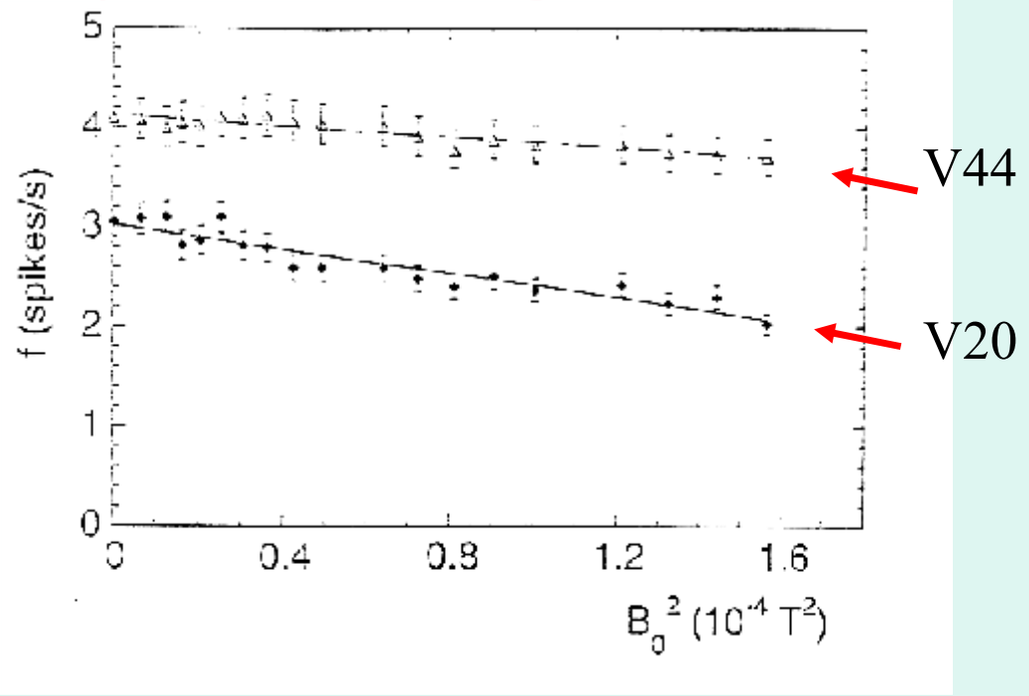

Fig.16.- Linear dependence of firing frequency with B^2_0 for couple of neurones V20 and V44 under 50-Hz applied AC magnetic field

From the slopes (α) of Fig.16 we find:
$N_c \approx 10^{12}$ PP/ cluster : ***neurons*** **become correlated** under ELF-MF, $N_c \approx 10^4$ ***times bigger than under weak static MF*** !.
Huge **size PP clusters** are in some way acting ***cooperatively***!.

♦♦ Neuron firing ***Synchronization***:

- ***Most remarkable is that under ELF-MF neurons become synchronized, firing at same frequency f*** (Fig.17):

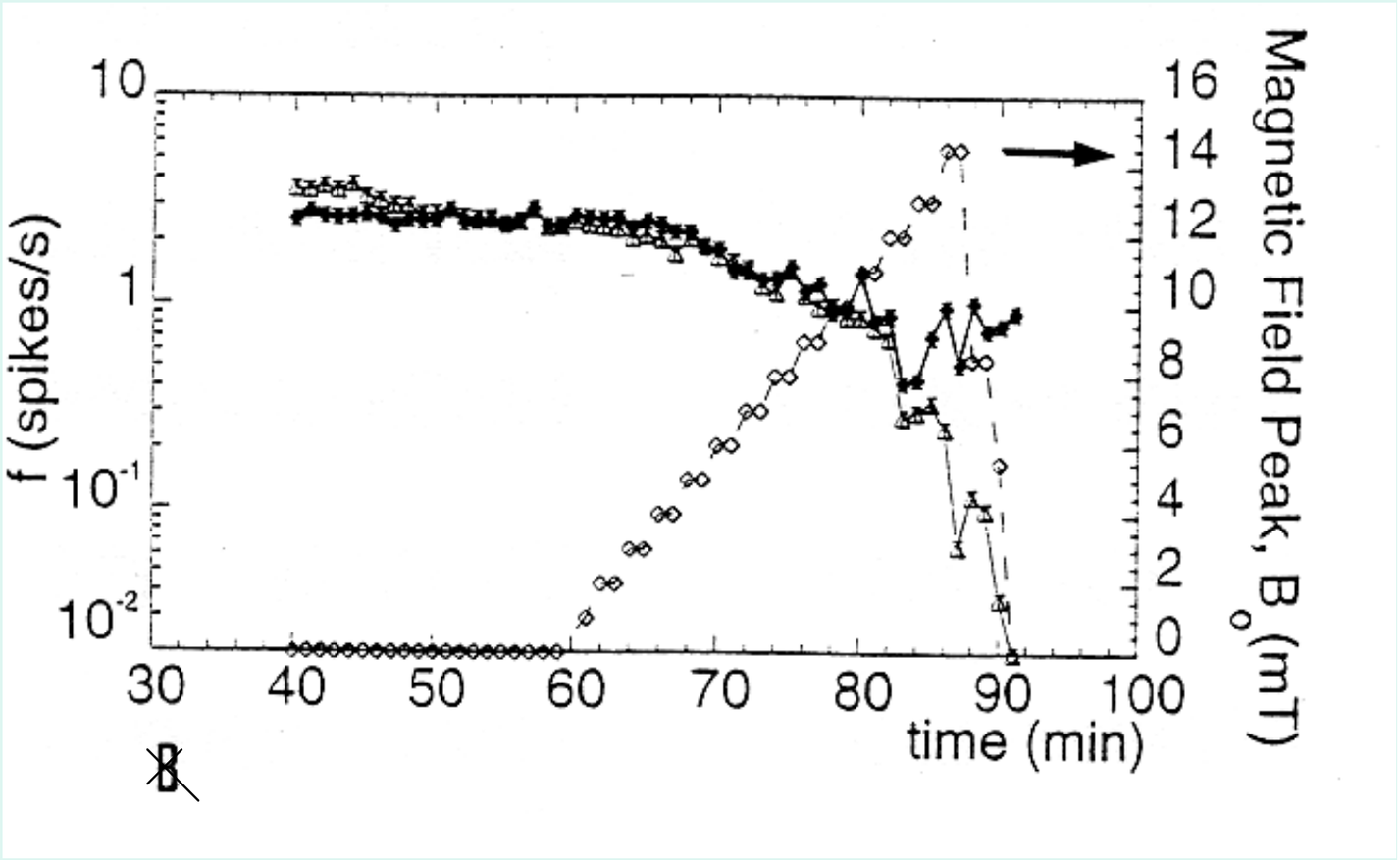

Fig.17.-Synchronization of firing frequency of pair of neurons V20-V44 under applied **50 Hz**-AC MF. *The induced synchronizing activity remains for about* ***32 min***. The frequency for both neurons decreases as SMF increases, the full *f* variation is of about two orders of magnitude.

Cluster sizes under weak ELF AC MFS: small neurones networks:

◆ Only **adjustable parameter** is the cluster PP number, N_c in neurone. This can be obtained by determining the parameter α from the ***slopes***,

$$s = f(0)\alpha/2$$

of the $f(B_0)$ plots under $\mathbf{f_M = 50\ Hz}$ AC MF field (1,10).

Taking , $\chi_\perp \cong -0.56\times10^{-7}$ determined in erythrocyte membranes by combined SQUID magnetometry ($\Delta\chi$) and ($\chi_\perp$) electrophysiological experiments (5,19), $V \approx 5\times10^{-28}\ m^3$, $T \cong 293K$ and α values, we respectively obtain: $\mathbf{N_C \approx 4}$ **and 1 x10^{12} PP in a cluster**, which correspond to:

42 and 16 neurones in the clusters, forming **small *sychronized networks* under AC MF.**

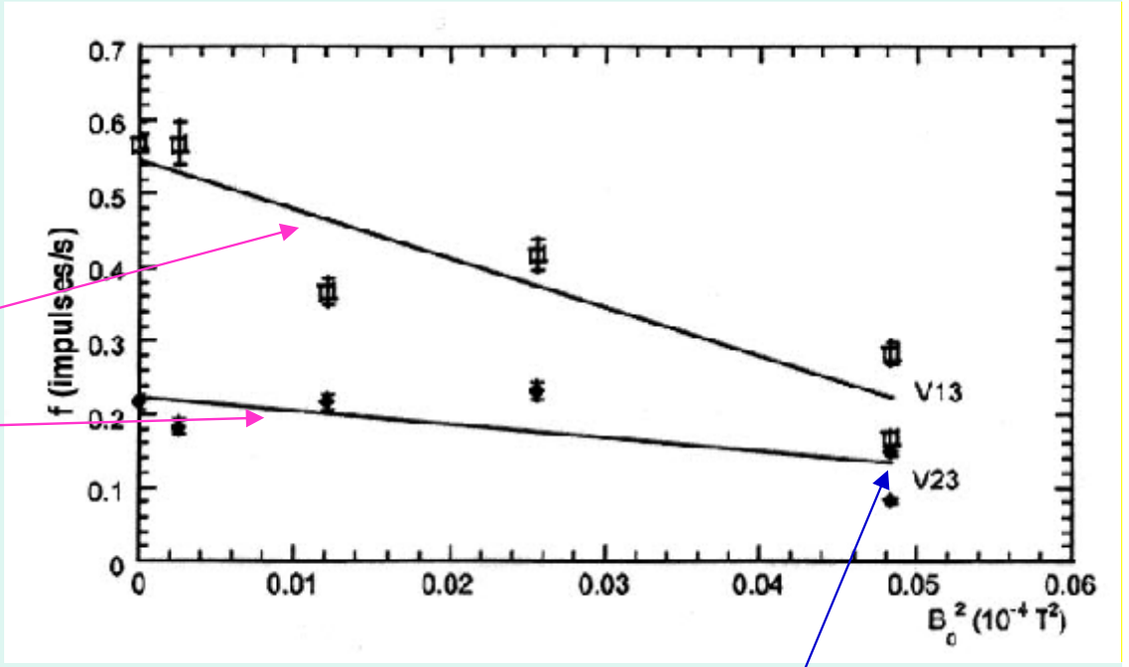

Fig.18.- *Helix aspersa* neurone pair V23-V13 (14), showing ***frequency synchronization*** **under AC MF** of f_M =50 Hz . From line slopes is determined the α parameter (for 56% studied neurones) (1) (10).

(1) Azanza M.J., and del Moral A., J. Magn. Magn. Mat. 157: 593 1996. (10) Ibidem.177:1451,1998.
(5) del Moral A., and Azanza M.J. J. Magn. Magn. Mat.114: 240-242, 1992.
(19) Azanza M.J., Blott B.H., del Moral A. and Peg M.T., Bioelectrochem. Bioenergetics, 30: 45,1993.

❁❁ *Synchronization volume:*

-PP numbers in clusters of synchronized neurones V20 and V44 are N_c= 2.1 and 1.1 x 10^{12} respectively, meaning synchronized clusters of about 13 and 7 neurones respectively, around probe ones.

- These numbers closely agree with NN neurone membranes around such a probes, for which quadrupolar interaction should be strongest: **atonishing result!.**

-Synchronization also found in V-ganglion pairs: 6-16, 7-59, 9-55, 13-23, 14-35, 15-49, 24-45, 25-27, 31-42, 41-54, 44-20, 46-47, 47-49, 48-64, 51-52, 53-61, 57-58.

-However, pairs are not NN, which means a ganglion generalized sychronization under AC MF!.

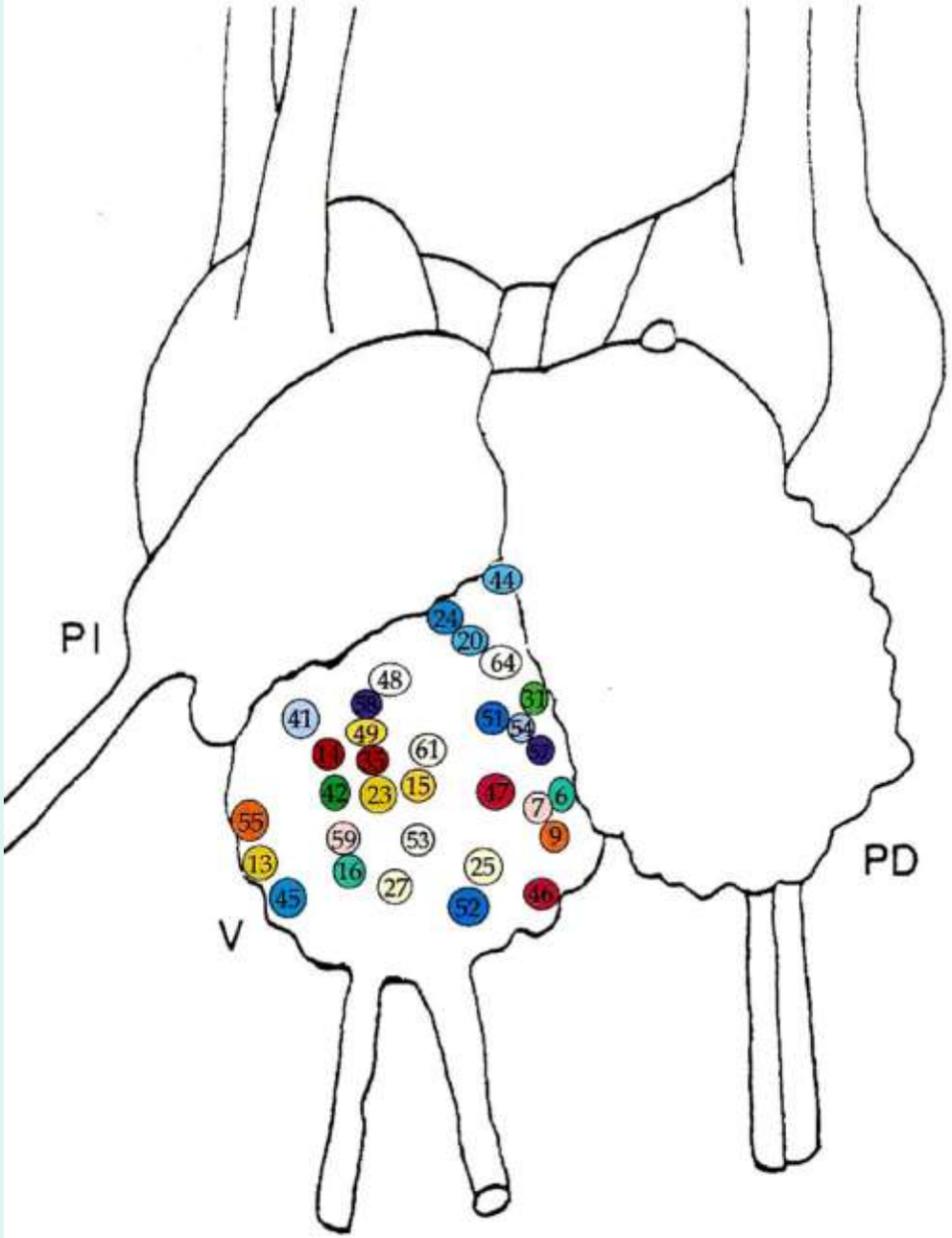

PART II.-

MODELS OF NEURONE DYNAMICS: SPONTANEOUS AND UNDER ELF ALTERNATING MAGNETIC FIELDS

CONTENTS

1.Bioelectric impulse shape and frequency spectrum: model based on modified Hodgkin&Huxley (HH) eqs. under AC ELF magnetic field: HH magnetic eqs.

● All those impulse **phases** can be explained by the **direct** ***integration*** of the **Huxley & Hodgkin (HH) equations** (3), **supplemented by the MF produced Ca^{2+} current (HHM eqs.)**, that we have done by assuming the membrane as a **Kirchoff *electric knot***, instead of as a parallel conductances network as done so far (4). Such an integration has ***not*** been apparently fully performed so far, the solution being partially *conjectured* (1).

●● Regarding to the second issue, the neuron impulse **frequency, *f* strongly changes** with the AC MF **frequency, f_M**.

●●● With SD+CE and HHM models we have conformed a **full picture** of the single unit neurone bioelectric behaviour, either for **spontaneous regime or under AC MF**, this of **extremely low frequencies (ELF)**.

(1) See e.g. R. Dodla & J. Rinzel, Phys.Rev.E 73 ,R10903 (2006); J. Lee et al., J.Theor.Biol. 242,123 (2006); K.A. Lindsay, J.R. Rosenberg and G.Tucker, J.Theor.Biol., 230: 39-48, (2004).

(3) Hodgkin A. I. and Huxley A.F. J.Physiol. 117: 500-544, 1952.

(4) Kandel E.R., Schwartz J.H. and Jessell T.M. *Principles of Neural Science*. McGraw Hill, New York, 2000.

♦*Biolectric impulse:*

- The process by which the impulse starts it is thought to be the result of small sub-threshold voltages sum up to a **threshold voltage**, V_s where the **depolarization (D)** process starts, with the **entrance of Na^{2+} ions** to the cell, through **voltage activated** Na^+-channels.

** We will discuss here the **time shape of the impulse** once it is formed, dividing it in: **depolarization (D)** and **hyperpolarization** (**H**, due to **sorting out of K^+ ions** through delayed rectifier voltage-operated K^+-channels).

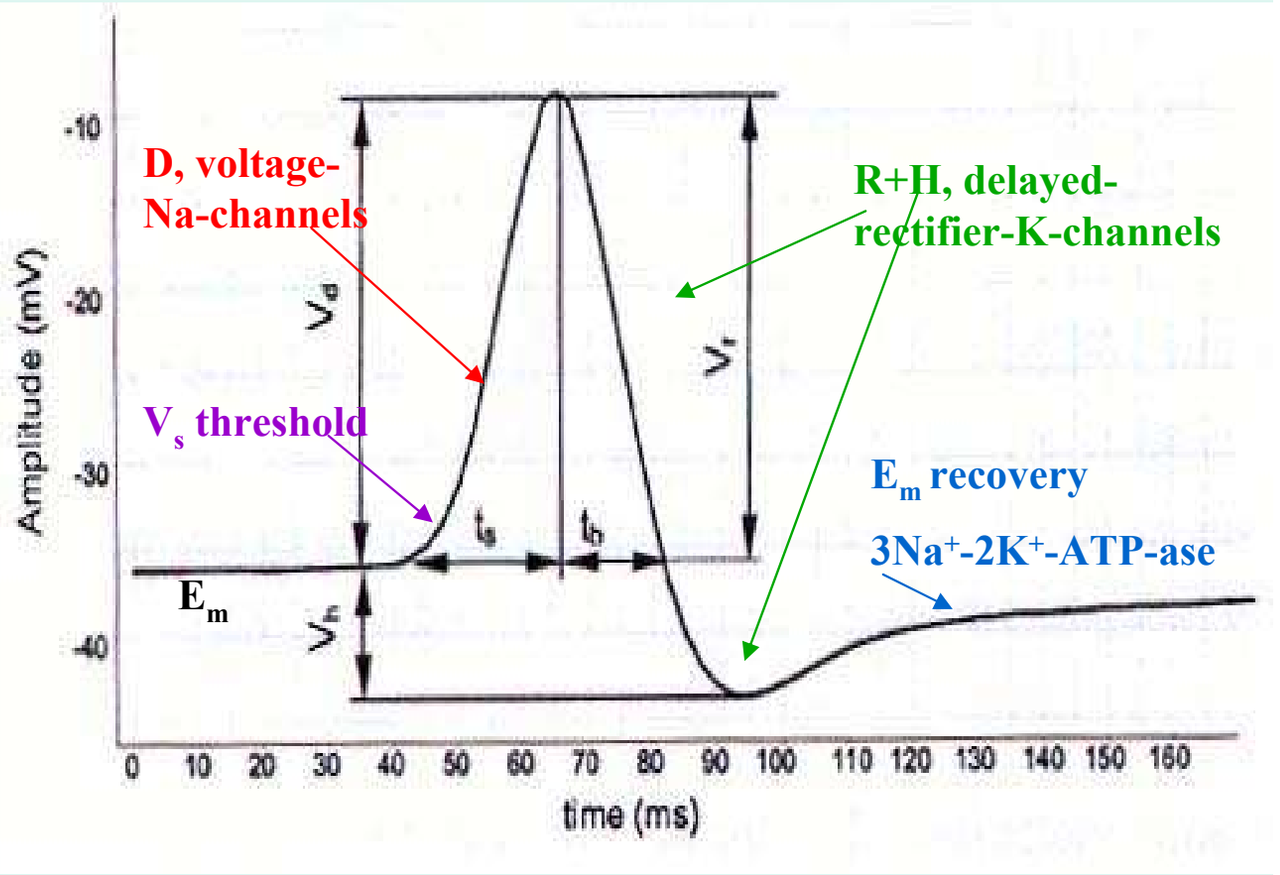

Fig.19.-

***The MF effect on **electrogenic pumps**,which promote the entrance of 2 K^+ ions against the sorting out of 3 Na^{2+} ions, making the membrane going to the **resting potential**, E_m was already considered in Part I, so completing the **full scenario**. The MF effect on such a regime is the **decrease** of impulse D amplitude, when MF is **strong** enough, as already explained (2).

(2) Azanza M.J., and del Moral A., J. Magn. Magn. Mat. 157-158: 593-594, 1996.

♦ ♦ Consideration of this network **by meshes does not allow its rigurous solution**, and we have considered the membrane as a **Kirchoff electric knot** where the currents concur.

Therefore **HH equation** takes the knot law of charge conservation (no charge accumulation in membrane),

$$C_m(dV/dt)+g_{Na}m(t)^3h(t)(V-E_{Na})+g_K n(t)^4(V-E_K)+g_L(V-V_L)-I_{Ca}(B_{eff},t)=0 \quad [1]$$

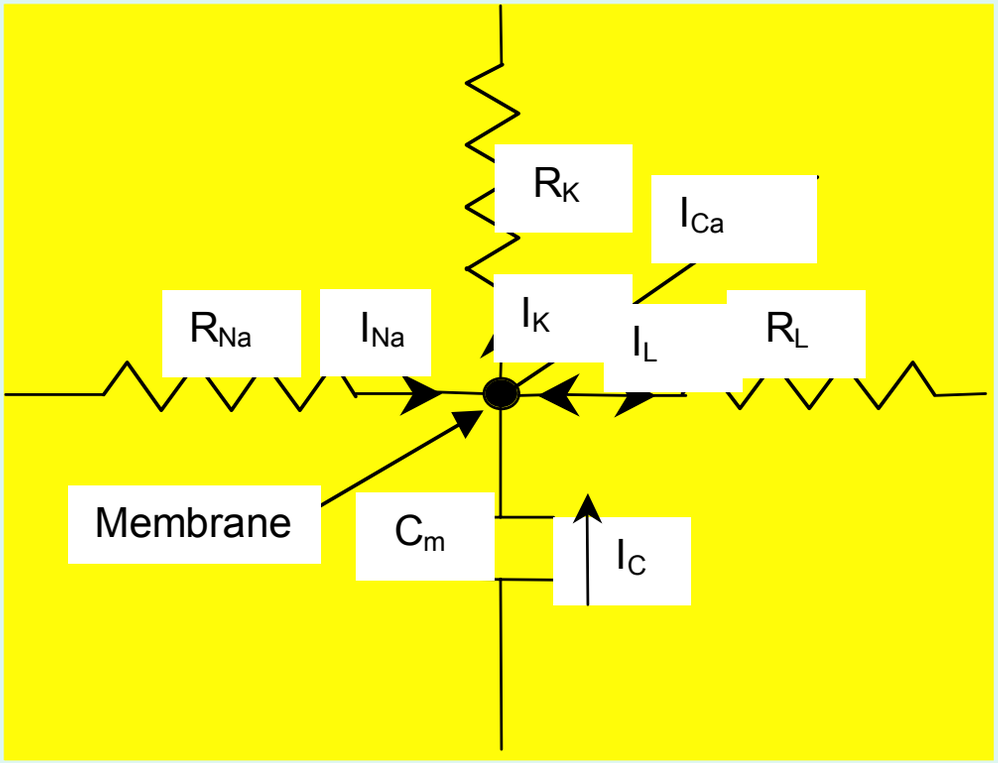

Fig.20.- Membrane equivalent Kirchoff electric knot.

where V is the transmembrane voltage, g_i (i = Na, K, L) the channels conductances. **m and n are the HH channel excitatory and h the inhibitory functions**, of microscopic origin not yet fully understood, although the phenomenologically needed **powers four**, point out to **four independent processes**, acting for the opening (m, n) and closing (h) of corresponding channels.

►Leakage (L) channels and ligand operated channels are likely responsible for the setting of the threshold voltage, V_s but current through them is weak and here **neglected**.

♦♦♦ Finally, HH currents **have been supplemented by the Ca^{2+} current produced by AC MF (**called ***HH magnetic*** **(HHM) equation).**

♦♦♦♦ Moreover under AC MF, the H process (where the cytosol becomes more negative due the K^+ ions sorting out) is modified by the **Ca^{2+} ions (in number of four, Fig.6) binding to the Ca^{2+} operated K^+ protein-channel** (more specifically to the calmodulin "gate" molecule) and opening it due to the **calmodulin electrical unfolding** (9). This explains the "power four" of HH function n(t).

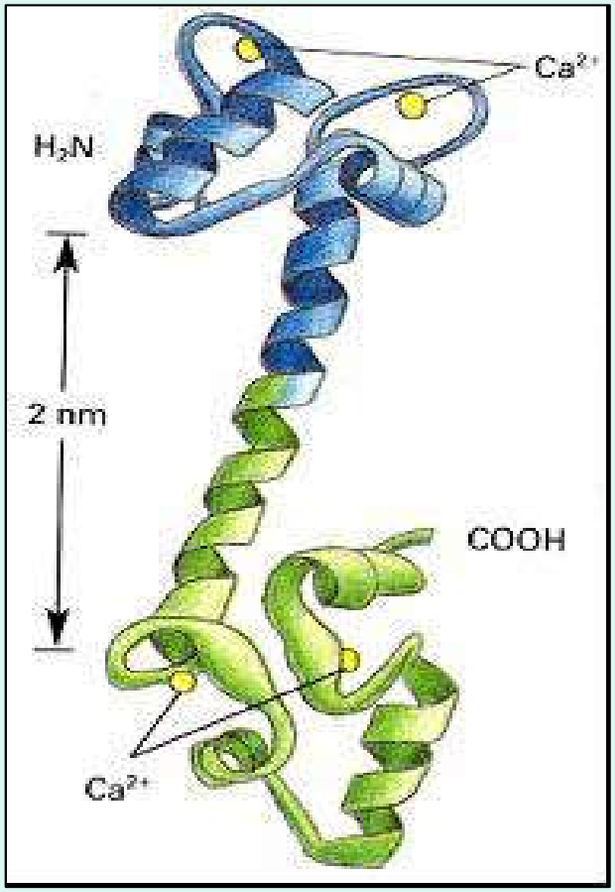

Fig.21.-

(9) Babu Y.S., Sack J.S., Greenough T.J., Bugg C.E., Means A.R. and Cook W.J. Nature. 315: 37-40, 1985.

♦♦♦ We have solved HHM eq.[1] in the ***relaxation time, τ, approximation*** for the HH functions, where e.g. for **excitatory n(t)**

$$dn/dt = -n(t)/\tau_K \qquad [2]$$

where n(t) is assumed to be **proportional to the number of K^+-channels which remain closed at time t**.

► Integration of eq.[2] taking t = 0 at the **beginning** of repolarization (R) plus H process, yields $n(t) = n_0 \exp(-t/\tau_K)$

Similarly taking t = 0 at the **beginning** of **D process** we obtain that excitatory

$$m(t) = m_0 \exp(-t/\tau_{Na}) \quad .$$

► In the other hand the **inhibition** function at **D process** follows the equation

$dh/dt = +h(t)/\tau_{inh}$, of integral $h(t) = h_0 \exp(+t/\tau_{inh})$, time increasing.

We will now obtain the **membrane voltage V(t) dependence**, partitioning the impulse in the mentioned regimes.

Repolarization and hyperpolarization:

✦ These two processes follow one after other and it is well known that in the **R+H process only K^+-channels** are open and therefore knot eq.[1] becomes,

$$C_m(dV/dt)+g_K\,n(t)^4\,(V-E_K)-I_{Ca}(B_{eff},t)=0$$

which integration after substitution of n(t) yields

$$V_K(t)=E_K+(E_{Na}-E_K)\exp\left[-(g_K n_0^4\tau_K/4C_m)(1-e^{-4t/\tau_K})+\int_0^t dt' I_{Ca}(B_{eff},t')/(V_K(t')-E_K)\right] \quad ,[3]$$

which is a complex **integral equation** with "kernel " $I_{Ca}(B_{eff},t)$ (t origin in eq.[3] is taken at $V(t)=E_{Na}$, origin of R).

Frequevy spectrum of R+H process:

✦✦ For comparison with experimental results in single neurones, it is useful to work in **frequency domain, ω,** so that we will obtain the ***frequency spectrum* of spontaneous impulse $V_K(t)$.** Fourier transform of eq.[3] exp[…] function is unknown, but for $t<\tau_K$ first exponential can be series expanded, so obtaining:

$$V_K(t)\approx E_K+(E_{Na}-E_K)\left[1-(g_K n_0^4\tau_K/4C_m)(1-e^{-4t/\tau_K})+\int_0^t dt' I_{Ca}(B_{eff},t')/(V_K(t')-E_K)\right] \quad [4]$$

✦✦✦ The ω **spectrum** of eq.[4] ***spontaneous*** $\mathbf{V_K(t)}$ ($I_{ca} = 0$) is obtained by Fourier transforming $V_K(t)$ around a central frequency ω_0^*, characteristic of the impulse (1st harmonic), yielding

$$V_K(\omega) = A^* \Big/ \left[\left(\omega - \omega_0^*\right)^2 + \left(\Delta\omega/2\right)^2 \right] \qquad [5]$$

where $A^* \equiv g_K n_0^4 \tau_K / 4C_m$ and

$$\Delta\omega/2 = 2\pi/\tau_K \qquad [6]$$

is the **HMHW, which provides τ_K.**

✦✦✦✦ Therefore the impulse spectrum is the well known ***lorentzian* function**, typical of resonance processes, taking its maximum value at $\omega = \omega_0^*$.

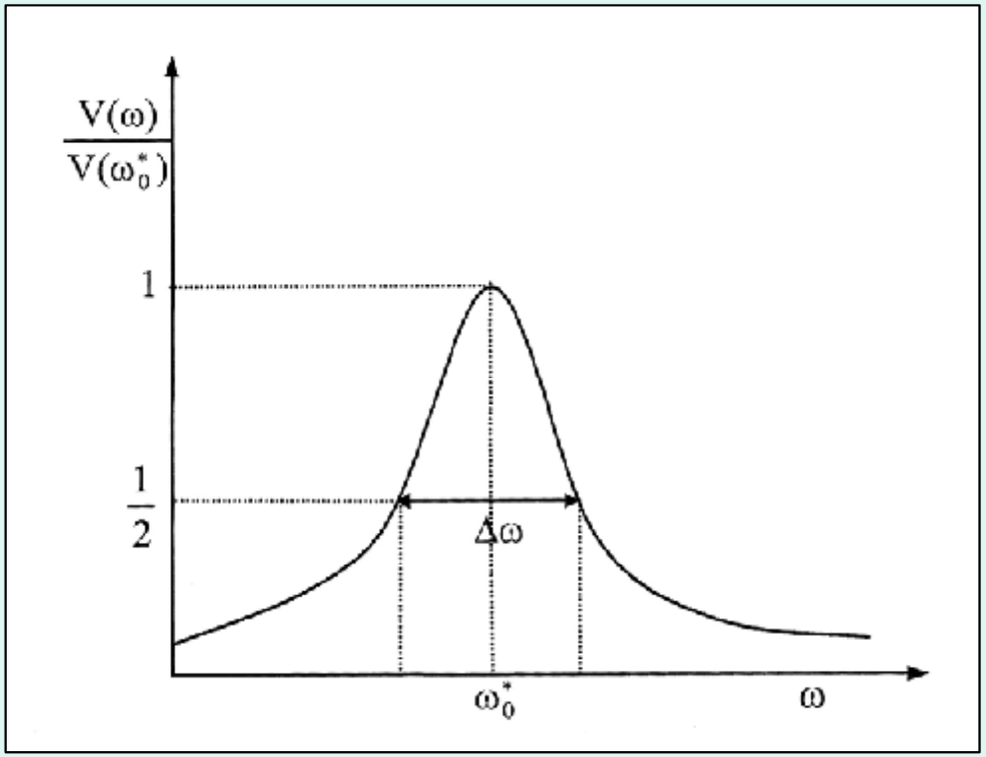

Fig.- 22

Eqs. for $V_K(t)$ and $V_K(\omega)$ can be easily extended to the real situation of having **different types of K^+-channels** (up to seven in *Helix aspersa* (13)), but this extension is not suitable for comparison with the impulse because of the too large number of parameters involved.

(13) Pérez-Castejón C., Junquera C., Pueyo A., Pérez-Bruzón R.N., Azanza M.J., Raso M., Pes N., Maestu C., Aisa J., Lahoz M., Martínez-Ciriano C., Vera-Gil A., and del Moral A. Histol. Histopathol. Suppl.1: S134, 2005.

Depolarization:

◎ This process follows after threshold voltage establishment, and since **involved Na^+ channels are operated by voltage**, inclusion of Ca^{2+} current only adds a term to $V_{Na}(t)$. But also **retarded in time K^+ channels are opened**, although being in small number during D tram their current **can be neglected**.

◎◎ The HHM relevant equation is then

$$C_m(dV/dt)+g_{Na}m(t)^3h(t)(V-E_{Na})-I_{Ca}(B_{eff},t)=0$$

which in presence of MF yields another integral equation. Integration followed by the **first exponential expansion** as before yields the **integral equation**,

$$V_{Na}(t)\approx E_{Na}\left[1-\left(g_{Na}m_0^3h_0\tau_{eff}/3C_m\right)\exp(-t/\tau_{eff})+\int_0^t dt' I_{Ca}(B_{eff},t')/\left(V_{Na}(t')-E_{Na}\right)\right] \quad , \quad [7]$$

where the **relaxation time** is given by $\tau_{eff}^{-1}=\tau_{Na}^{-1}-\tau_{inh}^{-1}/3$, since the inhibition and activation are independent processes.

◎◎◎ As before the ω-spectrum of spontaneous $V_{Na}(\omega)$ is **lorentzian** of HMHW $\Delta\omega/2=2\pi/\tau_{eff}$, and $A^*\equiv g_{Na}m_0^3h_0\tau_{eff}/3C_m$. Extension to different kinds of Na^+-channels is not worthwhile because of above mentioned reason.

Comparison with experiments in single neurones.

◆We compare our HHM model with electrophysiological experiments performed on *Helix* **single unit neurones.**

◆◆ Thus in Fig.23 we present the **spontaneous** ($B_{eff} = 0$) **R+H** potential time variation for two mapped neurones (14), fitted by the approximate solution for $V_K(t)$, the agreement being reasonable, but where *we do not reproduced the sigmoidal variation at the ends*, due to the **series cut-off in eq. for** $V_K(t)$.

◆◆◆ The more "accurate" frequently used **"sigmoidal" fit** by $\left(1 - e^{-t/\tau_K}\right)^4$ is also shown, but its basis upon n(t) is **phenomenological**, i.e. taking

$C_m = 0$, , $n(t) = n_\infty\left(1 - e^{-t/\tau_K}\right)$ and $V(t) \propto n(t)^4$

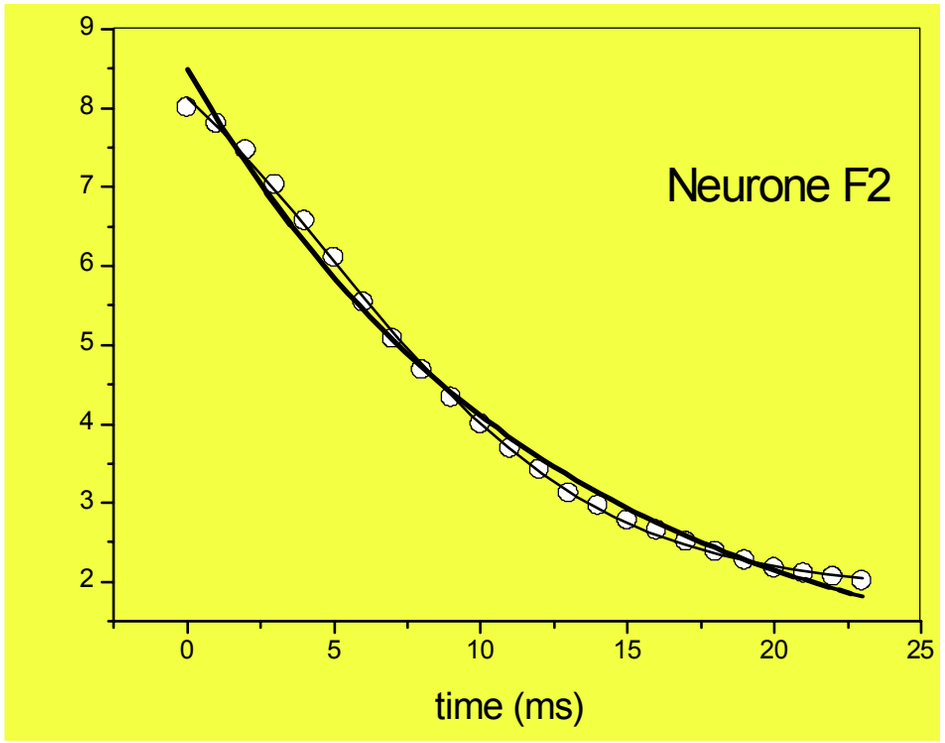

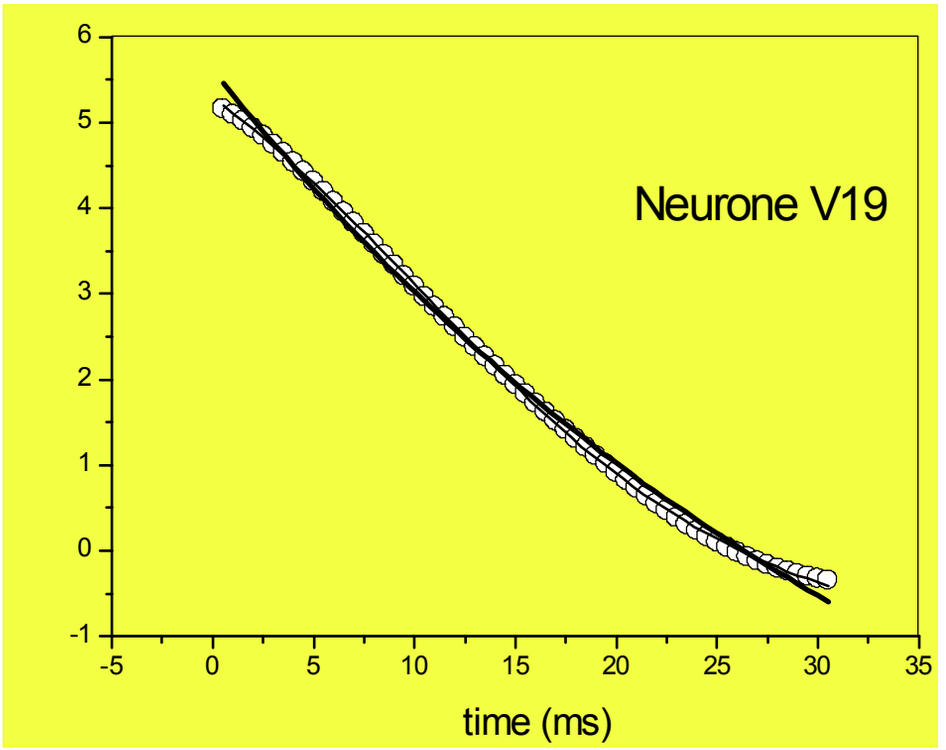

Fig.23.- Experimental (o) and model (thick line) R+H time variations; sigmoid (thin line).

◆◆◆◆ We now take , E_K = -75 mV, E_{Na}=+50 mV (this e.m.f. ***rectified*** by the delayed K^+ channels), $g_K = 1.6 \times 10^{-7}\,m^{-2}\,\Omega^{-2}$ and $C_m = 4 \times 10^{-2}\,Fm^{-2}$, and **from the fits we obtained the n_0 and τ_K values** quoted in Table 1

◆◆◆◆◆ Clearly we can **not** identify initial values n_0 with the number of K-protein channels (KP), with a density of $\approx$ 7 KP/μm^2, which for a neurone of 100 μm diameter yields $\approx$ **$2x10^4$ K-protein channels!.**

Table 1.- Initial values of HH function n(t) and K^+ relaxation time for several single neurones of *Helix*.

Neurone	n_0	τ_K (ms)
F1	200	33.0
F2	188	49.4
V3	202	45.0
V14	272	12.4
V19	155	156.7

Frequency spectrun of R+H impulse tram:

■ In Fig.24 we show the **frequency spectrum** of a bioelectric impulse of neurone V19, together with the fitted theoretical one by eq. for $V_K(\omega)$.

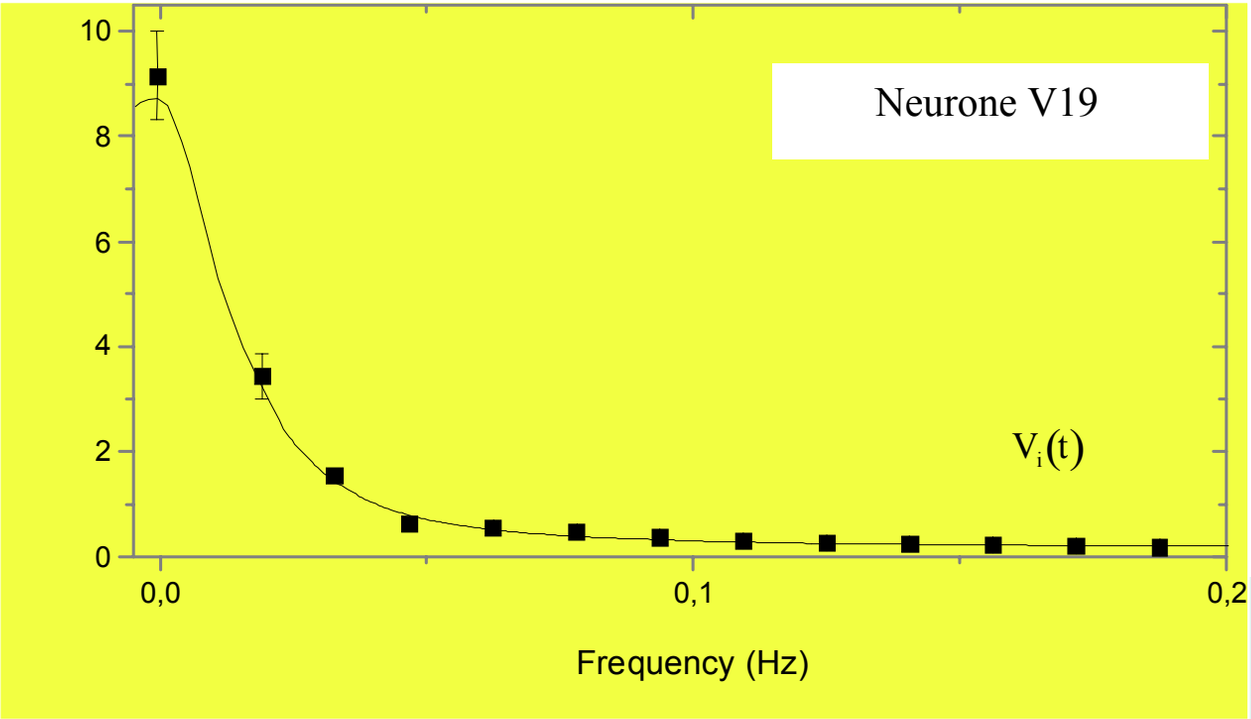

Fig.24.- Frequency spectrum of R+H tram impulse. Experiment (■) and **model fit (full line).**

■■ Using the **parameter values of Table 1** the agreement is excellent, the same happening for other studied neurones.

■■■ Under **applied weak AC MF** we have observed that **shape** of the impulse becomes practically ***unmodified***, which means that the solution of **full** integral eq. with $I_{Ca}(t)$ term is only required for **strong** MFs. Simplified **integral** eqs. for $V_i(t)$,i= K, Na can be transformed into second order linear **differential** equations,

$$\frac{d^2V_i}{dt^2} + C_i\left(\frac{n_i}{\tau(i)}\right)^2 e^{-t/\tau(i)} + I_{Ca}(t)\frac{dV_i}{dt} - (V_i + E_i)\frac{dI_{Ca}}{dt} = 0\,, \quad i = K, Na \qquad [8]$$

where: $C_K = g_K n_0^4 \tau_K / 4C_m$, $C_{Na} = g_{Na} m_0^3 h_0 \tau_{eff} / 3C_m$, $n_K = 4$, $n_{Na} = 1$,

$\Delta E_K = E_{Na} - E_K$, $\Delta E_{Na} = E_{Na}$, $\tau(K) = \tau_K / 4$, $\tau(Na) = \tau_{eff}$.

■■■■ This is an ordinary 2nd order differential equation of known solution of the kinds

$$V_i = A_i e^{\gamma_\pm(t)t} + B_i e^{\alpha_i(t)t}, i = K, Na \qquad [9]$$

where $\gamma_\pm(t) = (1/2)\left[-I_{Ca} \pm \sqrt{I_{Ca}^2 + 4(dI_{Ca}/dt)}\right]$ are the roots of homogeneous secular equation and α_i the exponent for the inhomogeneous one .

■■■■■ Therefore time dependence of H+R and D voltages are **theoretically rather complicated** in the **presence of an AC MF.** However **experiment says that the impulse shape does not significantly change in the presence of a weak AC MF** (usually 0.1-1 mT in our experiments, and down to 0.1 μT). May be impulse shape should change under ***much stronger AC*** MF, a matter to be investigated further.

Depolarization tram:

In **Fig. 25** are shown the D voltages for the **same neurones impulses**, fitted by eq. for $V_{Na}(t)$ using the above parameter values and $g_{Na} = 1.9 \times 10^{-7} m^{-2} \Omega^{-2}$, from the fits obtaining the values of $\left(m_0^3 h_0\right)^{1/4}$ and τ_{eff} quoted in above **Table 2.**

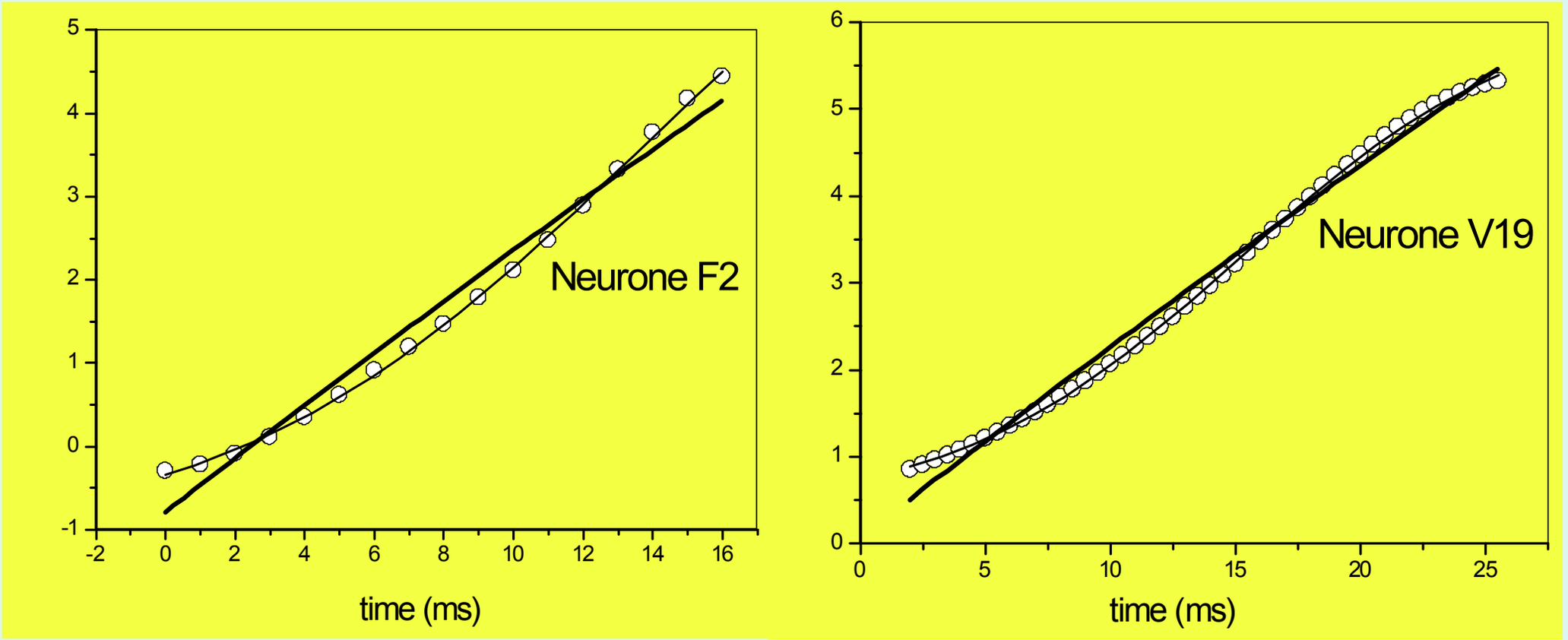

Fig. 25.- Depolarisation (D) voltage; (o) experiment; lines: **thick, model fit**; **thin, sigmoid.**

Table 2.- Initial values of m and h HH functions and D relaxation time, τ_{eff} for several single neurones of *Helix*.

Neurone	$\left(m_0^3 h_0\right)^{1/4}$	τ_{eff}(ms)
F1	51	92.7
F2	45	149.9
V3	45	109.6
V14	58	57.0
V19	41	222.8

- Values of $\left(m_0^3 h_0\right)^{1/4}$ are **larger** than n_0 ones, and same above consideration apply to them: they can **not** be the number of Na^+ protein channels, much larger.

- Also **sodium τ_{eff} are larger than potassium τ_K**, although in the impulse times $t_d < t_{r+h}$ because $V_{Na}(t)$ is interrupted at the smaller (abs.value) Nernst E_{Na} than E_K for $V_K(t)$.

Frequency spectrum of depolarization voltage:

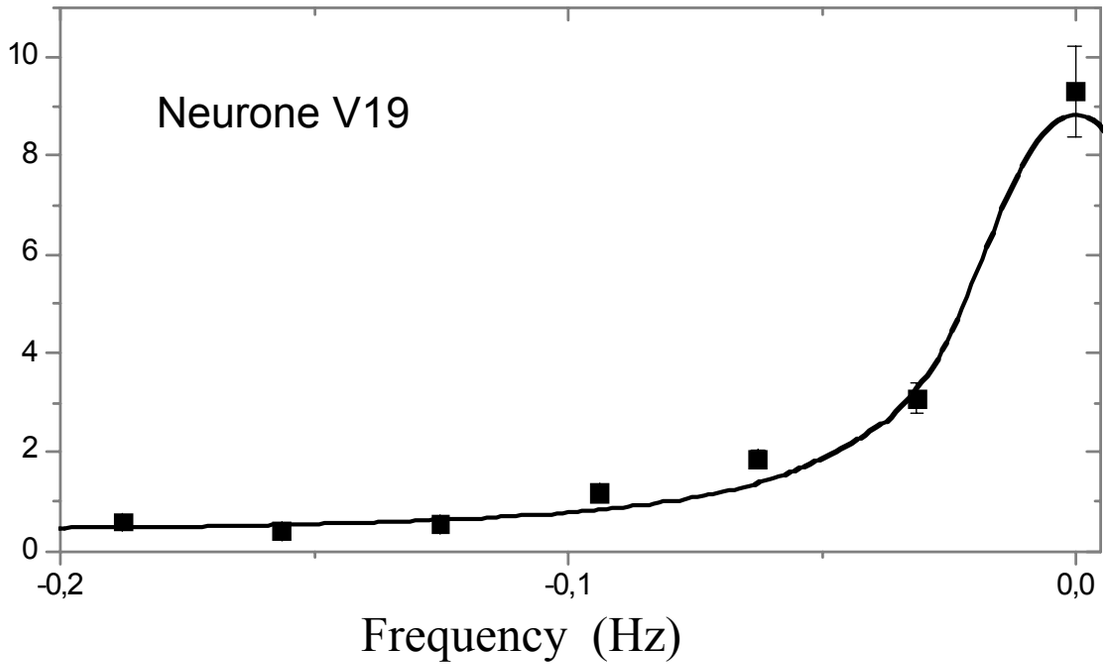

Fig.26.- Frequency spectrum (■) for impulse **depolarization** of neurone V-19. Line is the **lorentzian fit** $L(f)$.

- In **Fig.26** is shown the **frequency spectrum** of $V_{Na}(t)$ for neurone V-19, and the fit by the corresponding **lorentzian**, $L(f)$.
- ● D voltage is unmodified by applied **weak** AC MF and again solving of D equation under MF with I_{Ca} term is only needed for strong MF of $> \approx 1$ kOe

2.- Magnetic field frequency dependence of bioelectric activity: frequency window effect (FWE).

Previous background:

- In 1975 **Adey and co.** (15) prepared newborn **chicken brain** slices and embedded them in a physiological HCO_3^- water solution doped with radioactive $^{45}Ca^{2+}$ as marker. The tissue was then irradiated with a radiofrequency (RF) field of 147 MHz, ***amplitude modulated*** **by an ELF MF (of amplitude 25 - 30 nT) in the interval 0.5 - 35 Hz,** observing an **increase** of $^{45}Ca^{2+}$ efflux from the tissue. The experiments demonstrated two things:

i) **the RF (147 MHz) electromagnetic field (EMF) does *not* produce a measurable efflux increase (although a matter of current discussion);**

ii) a **calcium** efflux **increase** was observed for the tissue irradiated with the **ELF modulated wave**, but only within an interval of about **5-25 Hz**, so called ***frequency window*** effect (**FWE**).

(15) See Bawin S.M., Sheppard A. and Adey W.R., Bioeletrochem. Bioenergetics. 5: 67, 1978 and references therein; for further FWEs see M.J. Azanza and A. del Moral, Prog.Neurobiol. 44:517-601, 1994.

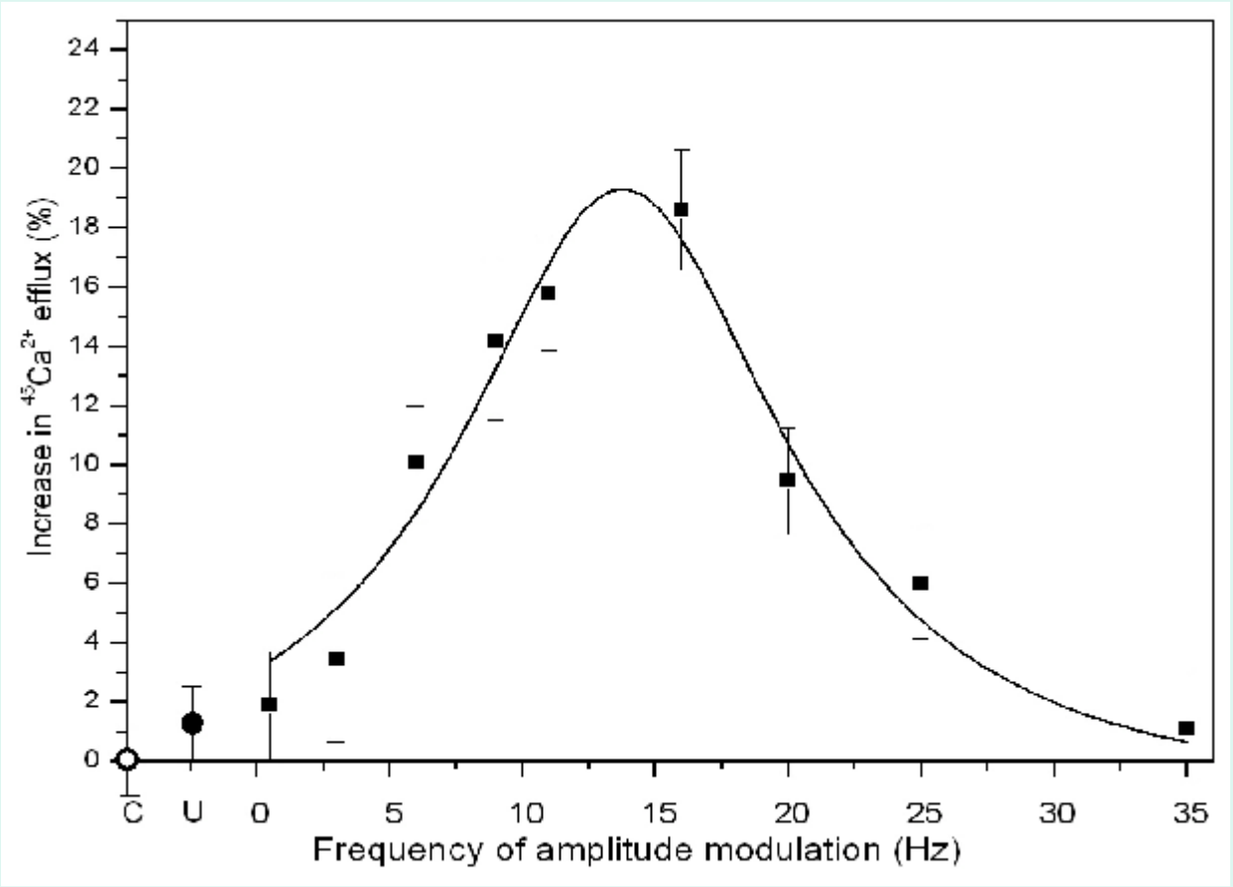

Fig.27.- The points (■) are the experimental $^{45}Ca^{2+}$ efflux increase from chicken brain under application of 147 MHz EMF carrier (intensity 0.8mW/cm^2), ***amplitude modulated*** by a MF of frequency, f_M between 0.5-35 Hz and $B_0 \cong 30$ nT (15). The **curve** is the **theoretical lorentzian**, **fitted according to our model lorentzian** (symbols C (O) and U (●) respectively correspond to sham and **unmodulated** EM-wave experiments).

(15) Bawin S.M., Sheppard A. and Adey W.R., Bioeletrochem. Bioenergetics. 5: 67, 1978.

● ● FWE was afterwards found in ***many other kinds of cells and experimental conditions*** (see **Azanza & del Moral, 1994** for a review), in particular:

⭘ for the **bioelectric *frequency*, *f* dependence** with the applied ELF **MF frequency,** f_M in *Helix* single neurones **(16)**, which constitutes our **current lecture**.

⭘⭘ We have also found a FWE in *Helix* brain neurones, irradiated with microwaves **of 9.6 GHz** (I< 75 mW/6 mm^2) ***amplitude modulated*** between f_M= 2-20 Hz, **but for the neurone firing frequency,** $f(f_M)$ ($\Delta f = 4$ Hz).

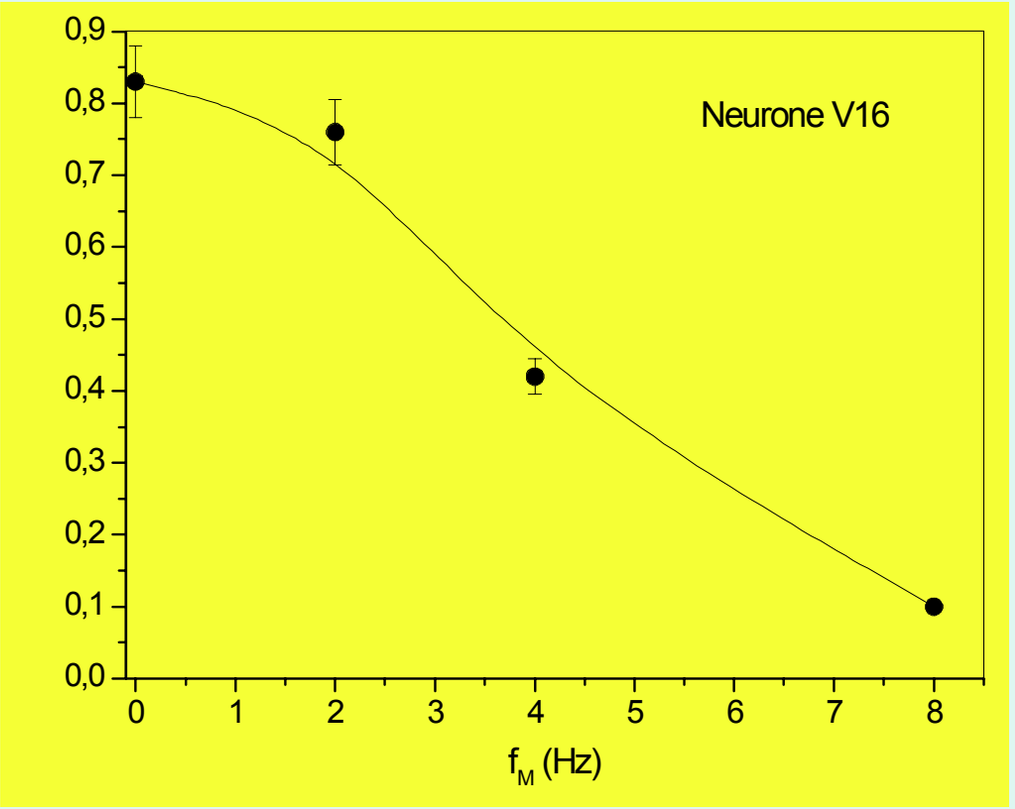

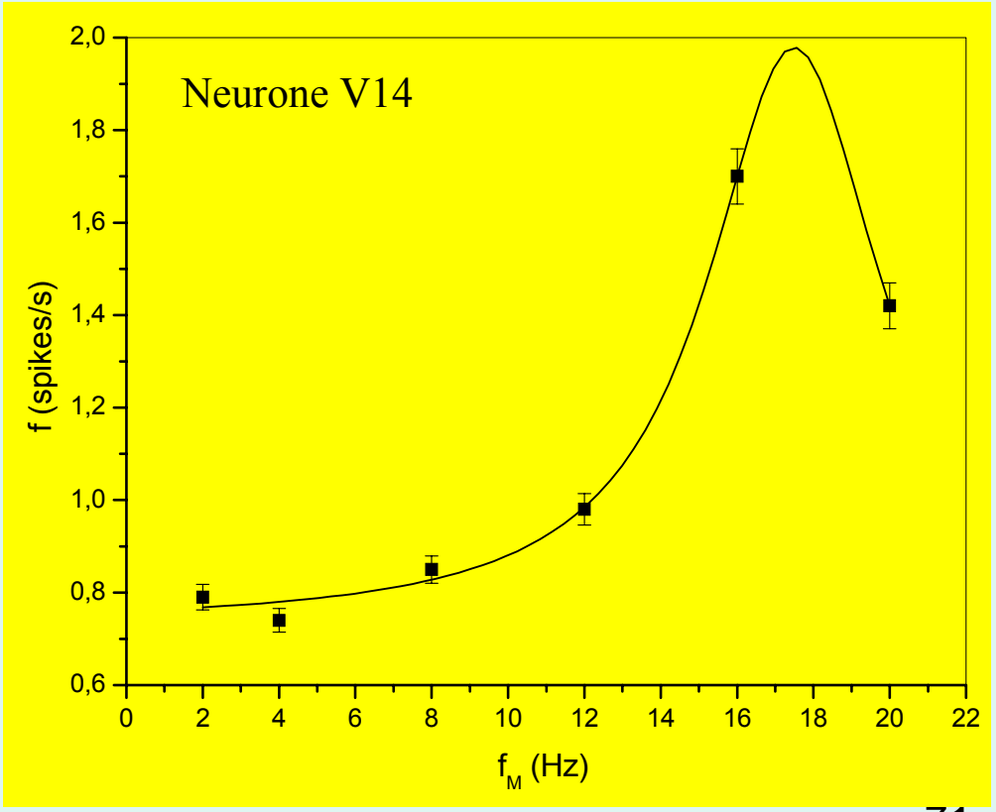

(6) Azanza M.J., and del Moral A. Prog. Neurobiol. 44: 517-601, 1994.
(16) Pérez-Bruzón R.N., Azanza M.J. And del Noral A. J.Magn.Magn.Mat.272-276:2424, 2004

Fig.28.-

Lorentzian dependence with f_M of Ca^{2+} efflux (Adey and co. experiment):

- Since Ca^{2+} electrochemical gradient, E_{Ca} displaces these ions to the cell interior, the observed efflux was interpreted as Ca^{2+} liberation from the **external** membrane surface.

- - Our **new observation** is that the calcium efflux closely follows a ***lorentzian*** curve, written now in the normalized form,

$$\phi(\omega_M) = \phi(\omega_0)(\Delta\omega/2)^2 \Big/ \left[(\omega_M - \omega_0)^2 + (\Delta\omega/2)^2\right] \quad , \quad [10]$$

where ω_0 is the frequency at the maximum efflux $\phi(\omega_0)$.

- Effectively, in Adey's Ca^{2+} efflux FWE the shown continuous line is the **fit by eq.[10]** to the experimental calcium efflux, and wher $f_0 = \omega_0/2\pi \cong 14$ Hz and $\Delta f = \Delta\omega/2\pi =$ 14.8 Hz.

Model for the FWE in sigle neurones:

♦ A quantitative explanation of such a FWE, although profusely mentioned and discussed since **1975** (6), **has remained unknown**.

♦♦ Although Adey and co. considered that the electric field of the ELF EMF was the responsible for the FWE, it is now clear that **it is the MF the responsible one** (16).

♦♦♦ Such a conclusion also stems from our experiments performed upon **single neurones** of *Helix*, submitted to an AC MF, of amplitude **0.1μT-1 mT** ,in the range of **0.1 - 80 Hz**.

♦♦♦♦ We have observed, for ≈56% of the neurones studied, a ***decrease*** in their bioelectric frequency, *f* ,with the ***increase*** of MF frequency, f_M ($\omega_M = 2\pi f_M$), and that the **frequency dependence** $\omega(\omega_M)$ **follows a *lorentzian* function as well**, i.e. there appears a **FWE for the firing frequency**.

(6) Azanza M.J., and del Moral A. Prog. Neurobiol. 44: 517-601, 1994.

(16) Pérez-Bruzón R.N., Azanza M.J and del Moral A. J. Magn. Magn. Mat. 272-276: 2424, 2004.

Origin of lorentzian spectrum or FWE:

- The *lorentzian* frequency, f_M dependence either of the calcium efflux $\phi(\omega_M)$ to the extra-cellular fluid, or the bioelectric frequency dependence, $f(f_M)$ in *Helix* neurones suggest a **common origin** for the time dependence of the **mechanism involved in the Ca^{2+} ions detaching** from their binding sites and their final sequestration or capture.

- This dependence merely is that the amount of Ca^{2+} ions either freed to the external or to the cytosol sides from the membrane ***must*** vary in the form

$$N(t) = N(0)\exp(-t/\tau_{Ca}) \quad , \qquad [11]$$

for an applied ELF MF starting at t = 0, solution of a dynamic equation of Ca^{2+} relaxation

$$dN/dt = -N/\tau_{Ca}$$

- This is so ***because the Fourier transform of a lorentzian function is an exponentially time decaying function*** (i.e. a **relaxation process**), with relaxation time $\tau_{Ca} = 2/\Delta f$.

- This is our **main point** for explaining **the FWE**.
- This is a ***very important observation***, ***signalling:***

why ELF-MF are the very significant ones for the interaction of neurons with quasistatic magnetic fields (1-100 Hz)!.

◆ The time τ_{Ca} is the one required for performing: the process of Ca^{2+} liberation from membrane, **mainly Ca^{2+} diffusion within the external or cytosol fluids** and final Ca^{2+} sequestration either by a protein channel or incoming to the radiactivity counter for the externally freed Ca^{2+} ions.

◆◆ For the Ca^{2+} ions freed to the extra-cellular fluid they will end up fully thermalized and dissolved in it, increasing its concentration ($^{45}Ca^{2+}$ efflux in **Adey & Bawin's experiment**).

◆◆◆ For the *Ca^{2+} ions liberated to cytosol*, they will **diffuse** and finally they will be captured by a K^+-protein channel through the calmodulin attractive electric field, $\mathbf{E}_{pK}$ (this field is active within the Debye length only!).

- The time τ_{Ca} is the one required for performing: the process of Ca^{2+} liberation from membrane, **mainly Ca^{2+} diffusion within the external or cytosol fluids** and final Ca^{2+} sequestration either by a protein channel or incoming to the counter for the externally freed Ca^{2+} ions.
- For the Ca^{2+} ions freed to the extra-cellular fluid they will end up fully thermalized and dissolved in it, increasing its concentration ($^{45}Ca^{2+}$ efflux in **Adey & Bawin's experiment**).
- For the *Ca^{2+} ions liberated to cytosol*, they will **diffuse** and finally they will be captured by a K^+-protein channel through the calmodulin attractive electric field, $\mathbf{E}_{pK}$.

◆◆◆◆ We can quantitatively express the above considerations by **Fourier transforming the observed lorentzian function** $L(\omega_M)$, which represents either the efflux $\phi(\omega_M)$ or the bioelectric frequency $\omega(\omega_M)$ dependencies, around the neurone spontaneous frequency, ω_0, i.e.

$$N(t)=\int_{-\infty}^{+\infty} L(\omega_M)\,\omega(B_{eff}=0)\exp(-\alpha B_{ef}^2)\exp(-i(\omega_M-\omega_0)t)d\omega_M =$$

$$\omega(B_{eff}=0)\exp(-\alpha B_{eff}^2)\int_{-\infty}^{+\infty}\frac{2(\Delta\omega/2)}{(\omega_M-\omega_0)^2+(\Delta\omega/2)^2}\exp(-i(\omega_M-\omega_0)t)d\omega_M = \quad [12]$$

$$\omega(B_{eff}=0)\exp(-\alpha B_{eff}^2)\exp(-t/\tau_{Ca})$$

Since the central frequency $\omega(B_{eff}=0)$ in [12] is assumed to be the spontaneous average bioelectric frequency, so we obtain a "***resonance***" or maximum of calcium efflux when $\omega_M = \omega_0$.

Calcium current:

- If we now recall that $[Ca^{2+}] = C/f\,(B_{eff},T)$ or the initially (at $t = 0$) detached Ca^{2+} ion concentration for a burst, **we end up with the Ca^{2+} time relaxation eq.**

$$I_{Ca}(B_{eff},t) \approx -(C' f_M\, q_{Ca^{2+}}) \exp(+\alpha B_{eff}^2) \exp(-t/\tau_{Ca}) = I_{Ca^{2+}}(B_{eff},0) \exp(-t/\tau_{Ca})$$

where $I_{Ca^{2+}}(B_{eff},0)$ is the initial Ca^{2+} current in a burst and τ_{Ca} **the Ca^{2+} relaxation time** (diffusion time in the cytoplasm).

- Since $\tau_{Ca} = \Delta\omega/2\pi$, which is experimentally accessible from the spectra $L(\omega_M)$,we can **determine that time from experiment.**

❖ In *Helix* brain neurones, repetitive **narrow bursts** of higher frequency, of **shorter duration with with f_M increase**, and superposed to the main $f(f_M)$ lorentzian decrease below f_0 (12), also are reminiscent of a FWE:

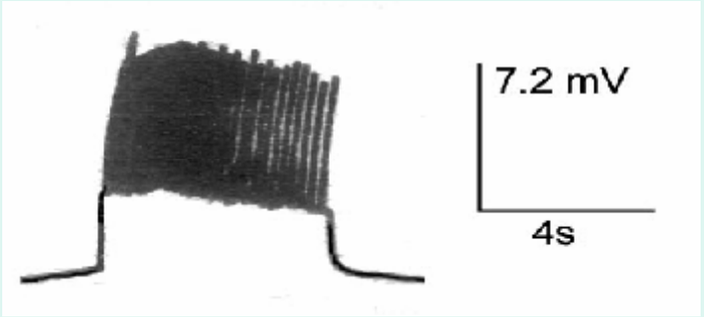

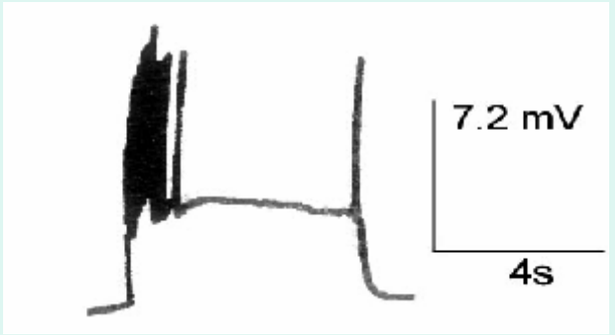

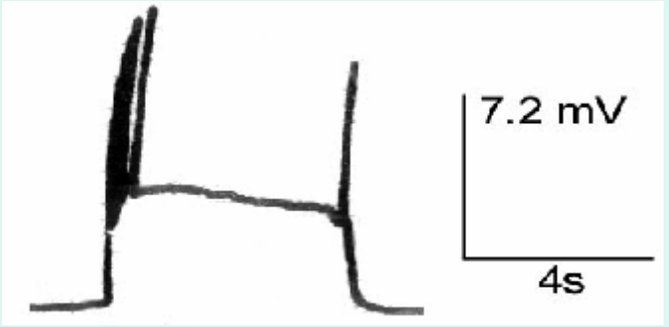

Fig.29.- f_M=0 Hz f_M=0.5 Hz f_M=1 Hz

❖ ❖ Note that the model distribution of **spontaneous** bioelectric frequencies, $D(\omega_0)$ (density of frequencies, setting $\omega_M = 0$ in $L(\omega_M)$) for the membrane, is also ***lorentzian***, extremely narrow, $\Delta f \cong 0.15\,\text{mHz}$

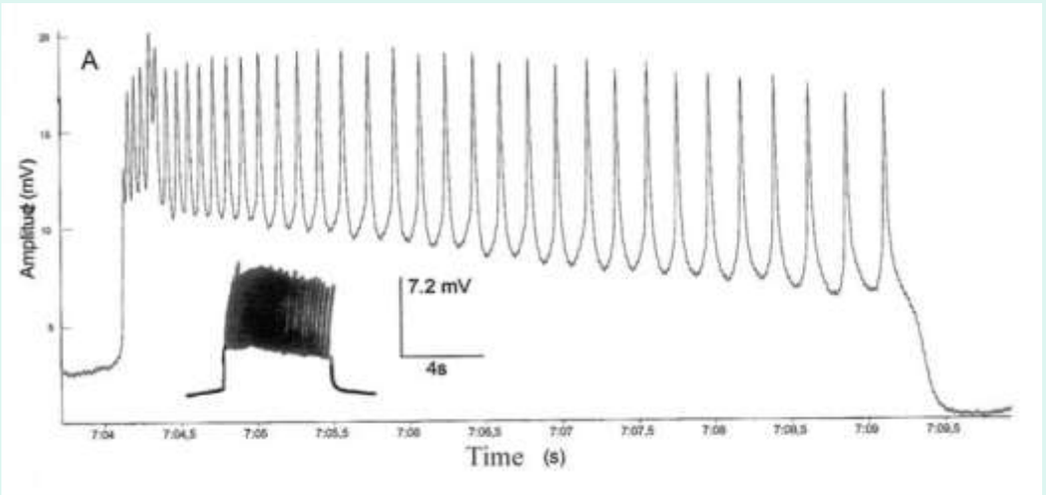

Fig.30.- Spontaneous burst

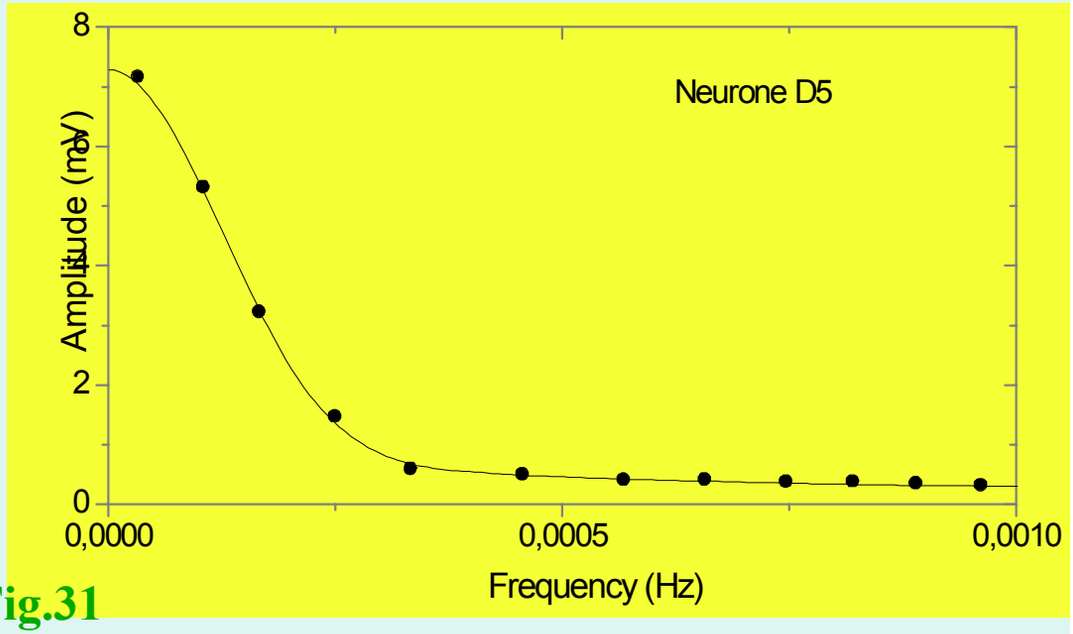

Fig.31

♦♦♦♦ The bioelectric frequency *f* vs. f_M variation for *Helix* brain mapped neurones F1 and V14, under AC MF of B_0=1 mT is very well fitted by a lorentzian $L(\omega_M)$

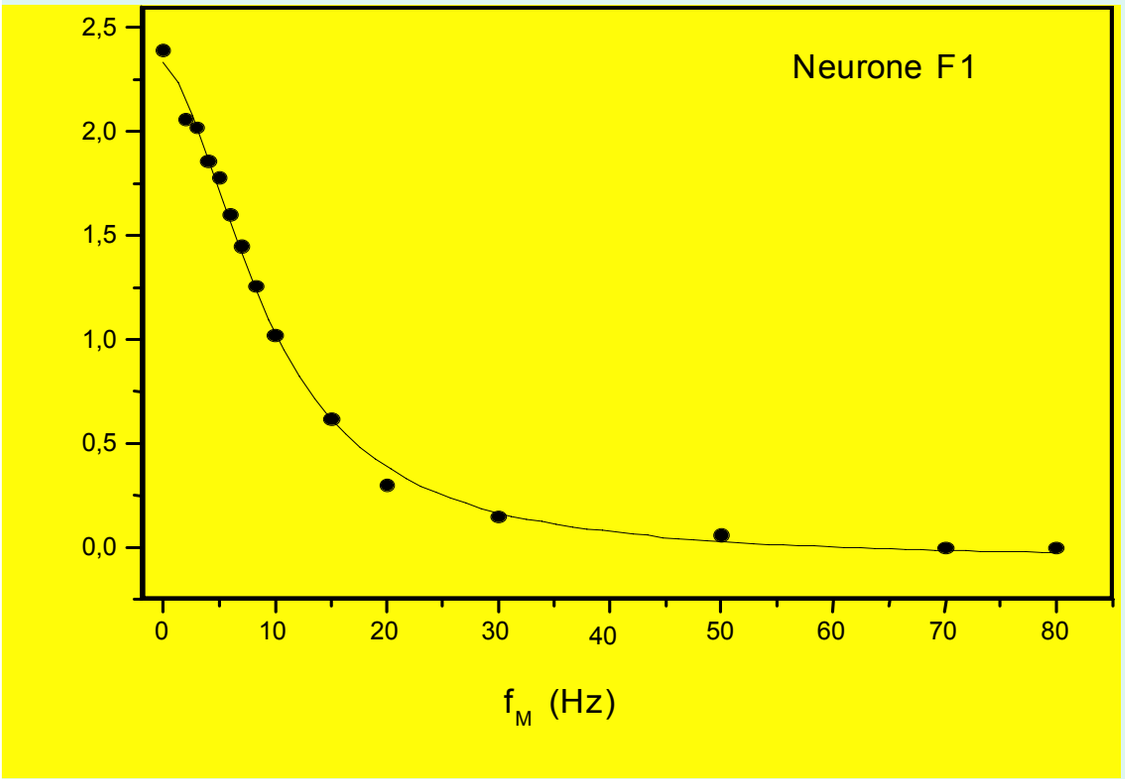

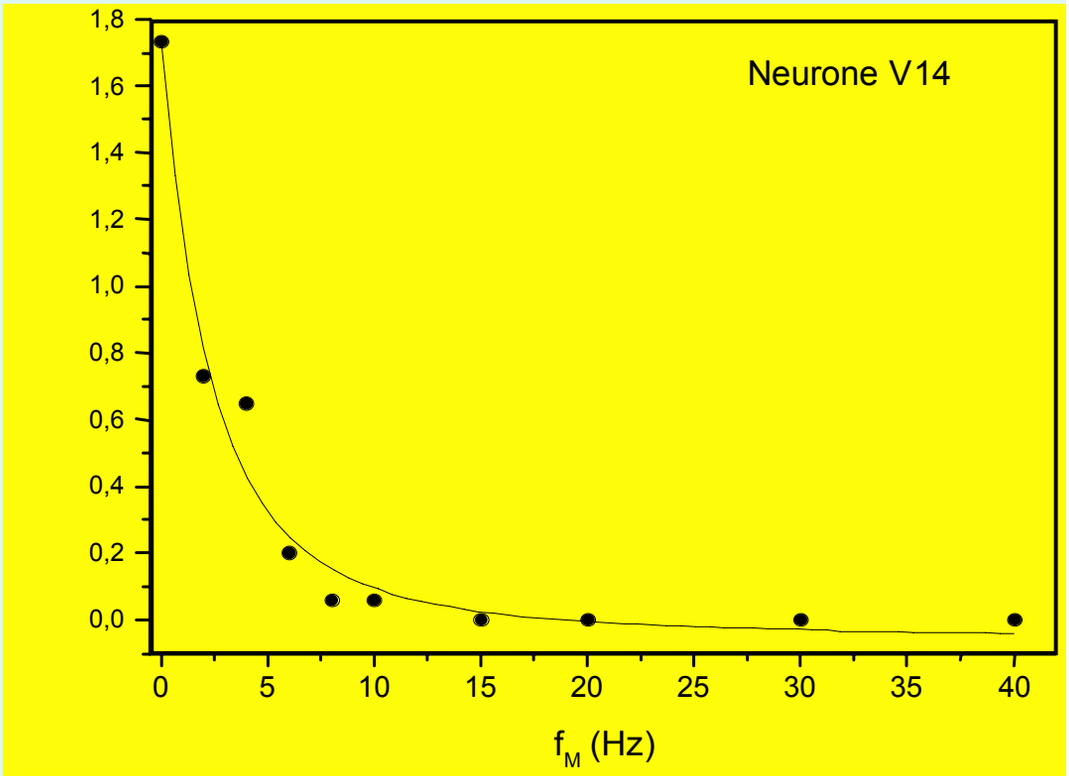

Fig.32.- Variation of bioelectric frequency, *f* with MF frequency, f_M. **Experiment** (●); **lines are lorentzian fits** $L(\omega_M)$ with f_0 =2.5, 2.0 Hz and $\Delta f/2$ = 9.9 , 2.7 Hz for neurones F1 and V14 respectively.

Ca^{2+} diffusion in the origin of lorentzian spectrum in neurones:

♦ Biolectric activity is *commanded by AC MF Ca^{2+} ions internally detached to the cytosol*, that join the K^+-protein channels and open them, giving rise to sorting out of K^+, or H+D process.

♦♦ Therefore this mechanism should be also operative in the chicken brain bioelectric activity, and therefore **all experiments reveal the Ca^{2+} simultaneous detaching from both surfaces of the membrane**.

♦♦♦ Besides the determined **Ca^{2+} relaxation times**, τ_{Ca} are **135 ms** (chicken brain) and between **93-365 ms** for the studied neurones of *Helix*. An *ab-initio* calculation of the Ca^{2+} relaxation time, τ_{Ca} is very difficult, if we consider the mentioned above kinetics involved.

(In fact a first principles calculation of the K^+ and Na^+ relaxation times in HH equations is still an open problem, relaxation times left as adjustable parameters as we showed before).

♦♦♦♦ However from τ_{Ca} we can estimate the mean diffusion length of Ca^{2+} in water, using Einstein's "annum mirabilis" (1905) eq. for a random walk (17):

$$\left\langle \bullet^2 \right\rangle = 6D\tau_{Ca} \qquad [13]$$

where ***D*** is Ca^{2+} **diffusion coefficient**. Taking $D \approx 10^{-9}\ m^2 s^{-1}$ the typical **diffusion coefficient** for small molecules in water (17), we obtain $\sqrt{\left\langle \bullet^2 \right\rangle} \approx 30 - 60\ \mu m$, reasonable values for the studied neurones of average **diameter d ≈100 μm** (1, 14).

(17) See e.g. Nelson P., *Biological Physics, Energy, Information, Life*, Freeman, New York, 2004.